Overdominance for fitness: A genomic comparison between empirical and simulated data with *Drosophila melanogaster*

Running title: Overdominance for fitness in Drosophila

Inés González-Castellano[1,2], Humberto Quesada[1], Sebastián Ramos-Onsins[3], Aurora García-Dorado[4], Armando Caballero[1*]

(1) Centro de Investigación Mariña, Universidade de Vigo, 36310 Vigo, Spain

(2) Universidade da Coruña, 15008 A Coruña, Spain

(3) Centre for Research in Agricultural Genomics CRAG (CSIC-IRTA-UAB-UB), 08193 Cerdanyola del Vallès, Barcelona, Spain

(4) Departamento de Genética, Facultad de Ciencias Biológicas, Universidad Complutense, 28040 Madrid, Spain

*Correspondence: armando@uvigo.gal

Abstract

Overdominance (heterozygote advantage) for fitness is a form of balancing selection which supports the maintenance of genetic polymorphisms in the populations. This mode of selection is expected to generate a conspicuous footprint on neutral genetic variation in genomic regions of restricted recombination, which contrasts with the signature generated by other types of natural selection. In particular, gene diversity is expected to be increased at neutral sites tightly linked to overdominant sites, as opposed to background selection and selective sweeps. We produced extensive whole-genome sequencing data to analyse genetic diversity across regions exhibiting varying recombination patterns in a *Drosophila melanogaster* population with known demographic history. The results were compared with simulation data in order to quantify the magnitude of the contribution of overdominant loci to genetic diversity which could be compatible with observations. We analysed sequencing data from 51 individual male flies sampled from a large population and estimated the average nucleotide diversity (π) in 100-kb consecutive windows across the main autosomal chromosomes. By using the available recombination map in the species, we evaluated the changes in π in relation with the levels of recombination across genomic regions. We then carried out computer simulations following the demographic history, the genomic architecture and the recombination map of the main autosomal chromosomes assuming models which include deleterious (background selection) and advantageous (selective sweeps) mutations, or models also including increasing rates of overdominant mutations. By comparing the results obtained from simulations and the observed data, we conclude that a parsimonious model of background selection and adaptation to captivity explains the observed patterns of neutral variation in the studied population better than the models including overdominance.

Keywords: heterozygote advantage, balancing selection, nucleotide diversity, inbreeding load, computer simulations, SNP.

Introduction

It is well known that selection shapes genomic variation at neutral sites linked to selective ones, the so-called linked selection hypothesis (Cutter & Payseur, 2013; Elyashiv et al., 2016). Thus, purifying selection against deleterious variants (background selection) and the spreading of beneficial mutations towards fixation (selective sweeps) reduce nearby neutral diversity (Berry et al., 1991; Maynard-Smith & Haigh, 1974; Charlesworth et al., 1993). Because lower genetic recombination implies tighter linkage, the effects of these types of selection on neutral linked variants are amplified in regions of low recombination, leading to the positive correlation between recombination rates and genetic diversity that has been reported in numerous species (Begun & Aquadro, 1992; Charlesworth & Campos, 2014; Comeron, 2014; 2017). However, heterozygote advantage for fitness, also known as overdominance, is a form of balancing selection that maintains alleles in populations as polymorphisms with stable frequencies (Kimura & Ohta, 1971). Furthermore, in gametes bearing different alleles at an overdominant site, the divergence at neutral sites is inversely related to $2N_ec$, where N_e is the effective population size (Wright, 1931), and c is the recombination fraction between the neutral and the overdominant sites (Hudson, 1990). Therefore, gene diversity is expected to be increased at neutral sites tightly linked to overdominant sites, as opposed to background selection and selective sweeps. Thus, the resulting signature of overdominance is that neutral variants linked to the balanced sites are also kept at intermediate frequencies in the populations, what is known as associative overdominance (Frydenberg, 1963; Pamilo & Pálsson, 1998; Comeron, 2014; Bersabé et al., 2016; Zhao & Charlesworth, 2016), generating an excess of neutral diversity relative to that expected in the absence of selection (Nielsen, 2005; Charlesworth, 2006).

True overdominance appears to be a rather rare genetic condition with only a few well-documented cases, such as sickle cell anaemia (Allison, 1956), immunity-related genes in humans (Bitarello et al., 2018; Minias & Vinkler, 2022), warfarin resistance in rats (Partridge, 1979), female fecundity in sheep (Gemmel & Slate, 2006), male horn size in sheep (Johnston et al., 2013), or productivity in *C. elegans* (Peters et al., 2003), among other examples in different species (see review by Hedrick, 2012). Overdominance can be generated by antagonistic pleiotropy affecting different fitness traits (Rose, 1982; Roff, 1997; Fernández et al., 2005), for instance, due to a negative relationship between reproduction and lifespan, as observed in many

vertebrates (Lemaître et al., 2015). In humans, an excess of genetic variants with opposing effects on early-onset and late-onset human diseases has also been found using genetic data (Rodríguez et al., 2017). In addition, genetic variants that have been favoured in the past may not be beneficial for some traits in the current environment, also generating antagonistic pleiotropy (Corbett et al., 2018). An extensive meta-analysis of selection coefficients reported in the literature from natural populations of multiple taxa found that about 2% of the coefficients examined showed overdominant behaviour (Thurman & Barrett, 2016). This figure should be interpreted with caution due to the low statistical precision of many estimates (Thurman & Barrett, 2016), and given that most genes showing heterozygous advantage in vertebrates were those classically known to be the paradigm of balancing selection, such as the *β-hemoglobin* and the major histocompatibility complex (*MHC*) / human leukocyte antigen genes (*HLA*). Thus, the role of overdominance in maintaining variation in the genome is expected to be restricted to particular genes and mostly confined to low-recombining regions (Draghi & Whitlock, 2015; Fijarczyk & Babik, 2015).

It should be noted that associative overdominance in regions of low recombination can arise not only from true overdominance, but also from complementation between recessive deleterious mutations at closely linked loci in repulsion phase, what is known as pseudo-overdominance (Ohta, 1971; Becher et al., 2020; Gilbert et al., 2020; Waller, 2021; Abu-Awad & Waller, 2023). The deleterious effects of haplotypes are masked in heterozygous condition, so that the heterozygotes appear to have the highest fitness, which can be mistaken for true overdominance (Waller, 2021). Because pseudo-overdominance mimics balancing selection, it allows neutral diversity to be maintained in regions of low recombination (Zhao & Charlesworth, 2016; Gilbert et al., 2020; Waller, 2021; Sianta et al., 2023), which may be crucial for small populations (Schou et al., 2017).

An excess of genetic variance has been found for different fitness traits relative to expectations from mutation-selection balance (Charlesworth, 2015; Sharp & Agrawal, 2018), which could be ascribed to balancing selection. Different studies have also shown that genomic regions subjected to balancing selection can be common (Andrés et al., 2009; Gao et al., 2015; Schou et al., 2017; Siewert & Voight, 2017; Bitarello et al., 2018; Wang et al., 2019; Gilbert et al., 2020; Soni et al., 2022). These episodes of balancing selection could be caused by pure

overdominance, pseudo-overdominance or other forms of balancing selection, such as frequency-dependent selection, selection pressures varying in space or time, or genotype-environment interactions (Lande, 1976; Rose, 1982; García-Dorado, 1986; Mukai, 1988; Roff, 1997; Santos, 1997; Charlesworth & Hughes, 1999; Charlesworth, 2006).

The detection of signatures of balancing selection, through a pattern of excess of common polymorphisms, can be made by different statistics, classically by Tajima's (1989) *D* or the HKA test (Hudson et al., 1987). Nonetheless, these methods have a low power and tend to be extremely sensitive to non-equilibrium demography or population structure (Fijarczyk & Babik, 2015; Siewert & Voight, 2017). More powerful statistics have recently revealed some evidence of balancing selection in the human genome. For example, Andrés et al. (2009) detected 60 genes with significant signatures of long-term balancing selection as shown by their excess of polymorphism and intermediate-frequency alleles. Likewise, Bitarello et al. (2018) indicated that long-term balancing selection in humans may be shaping variation in up to 2% of variable genomic positions. Moreover, Soni et al. (2022) provided evidence that hundreds of nonsynonymous polymorphisms in the human genome could be subject to balancing selection. However, all these evidences of balancing selection may be due to sources different from overdominance for fitness, as mentioned earlier, except perhaps for particular genomic regions, so it is unclear whether or not overdominance is a widespread phenomenon.

In addition to its effects on genetic diversity, overdominance has also been discussed in terms of its role on inbreeding depression, i.e. the decline in fitness-related traits observed in inbred individuals compared to their non-inbred counterparts (Keller & Waller, 2002; Hasselgren & Norén, 2019). Inbreeding increases genomic homozygosity, allowing the expression of the inbreeding load (*B*), which is the detrimental genetic burden that is concealed in the heterozygous state in outbred populations (Morton et al., 1956). This load can be attributed to the exposure of (partially) recessive deleterious alleles in homozygotes (dominance hypothesis) or to the homozygosity of loci with heterozygote advantage (overdominance hypothesis). A recent simulation study shows that the usual methods to estimate inbreeding depression from dominant loci are also applicable and precisely estimate inbreeding depression from overdominant loci (González-Castellano et al., 2025a). The relative contribution of these two sources of inbreeding load have been debated for decades (Charlesworth & Willis, 2009; Ayroles et al., 2009; Paige,

2010; Schou et al., 2018), although the current consensus is that partial dominance plays the major role in inbreeding depression, as supported by the majority of empirical and theoretical studies (Charlesworth & Charlesworth, 1987; 1999; Barrett & Charlesworth, 1991; Crow, 1999; Roff, 2002; Hedrick, 2012; Yang et al., 2017; González-Castellano et al., 2025b).

In this study, we set out to elucidate the possible contribution of overdominance to genetic diversity by contrasting genomic data with simulation results. We analysed whole-genome sequencing data from a laboratory population of *Drosophila melanogaster* with known demographic history to evaluate patterns of variability across genomic regions with contrasting recombination rates. The unusual circumstance that the recent demography of the population is known, allowed us to develop models to investigate the genetic architecture of the population. Thus, we performed computer simulations based on the population demography, genetic architecture and recombination map of the species, considering only neutral, deleterious and additive advantageous mutations, or also adding an increasing number of overdominant mutations, in order to assess whether the empirical data are compatible with the absence or presence of overdominance. We do not consider in the simulations other possible types of balancing selection, although pseudo-overdominance is also implicit in the models.

Materials and Methods

Experimental population

A *D. melanogaster* population was founded in 2009 from a wine cellar population and maintained with around 2,800 individuals as described by López-Cortegano et al. (2016) and Pérez-Pereira et al. (2021). The population was maintained with constant temperature (25ºC) and continuous lighting with circular mixing of 32 bottles (numbered from 1 to 32) each with 40-50 individuals of each sex and the feeding medium used in our laboratory (1 liter water, 200 g brewer's yeast, 50 g sucrose, 12 g agar, 2.5 g NaCl, and 5 ml propionic acid). In each generation, 20-25 individuals (about half of each sex) were taken from bottle i and the same number from bottle $i - 1$ (from bottle 32 in the case $i = 1$) to found bottle i of the following generation. Male and female adults in each bottle were removed after a week, before the next generation emerged, to avoid overlapping generations. At generation 208, after ~10 years of maintenance in the

laboratory with an approximately constant population size, a total of 51 males were sampled from the population to carry out individual whole-genome sequencing.

DNA extraction, sequencing and SNP calling

The sampled individuals were frozen in liquid nitrogen and stored at –80 ºC. An optimized protocol for DNA extraction from individual flies including treatment with RNase was carried out with the Gentra Puregene Cell Kit (Qiagen). Whole-genome sequencing of 2 × 150 bp paired-end was performed by Macrogen (South Korea) on an Illumina Novaseq 6000 instrument using Nextera XT DNA libraries. FASTQ sequencing files underwent a first quality control with FastQC (Andrews, 2010), and adapters were removed with Trimmomatic (Bolger et al., 2014) using Nextera adapter list. ERNE-FILTER v2 (Del Fabbro et al., 2013) was used to carry out quality and size trimming (minimum sequence length after trimming = 36). After a new quality control with FastQC, the obtained reads were mapped against the 6.14 *D. melanogaster* reference genome with BWA-MEM (Li, 2013). The resulting SAM files were converted to indexed BAM files with SAMtools v1 (Danecek et al., 2021), and chromosomes were isolated and indexed. SAMtools v1 was also used for PCR duplicate removal and filtering (minimum mapping quality = 20). Qualimap v2 (Okonechnikov et al., 2016) was used to perform the quality control of the alignment. The average sequencing depth and mapping quality were 43.49× (± 1.19) and 58.38 (± 0.01), respectively. Raw variant calling (minimum phred-scaled confidence threshold = 10) was carried out using the HaplotypeCaller tool from GATK v4 (Van der Auwera & O'Connor, 2020). The resulting gVCF files were combined using the GATK CombineGVCFs tool, keeping only biallelic SNPs. Highly repeated sites, low information regions, and SNPs within 10 bp of an indel were removed with BCFtools (Danecek et al., 2021). Finally, SNPs were also filtered with the GATK VariantFiltration tool applying the recommended presets. The final number of called SNPs was 1,541,774. Various filters were then applied to remove potentially selective SNPs. First, ANNOVAR v4.19 (Wang et al., 2010) was used to annotate SNPs into categories such as 5'UTR and 3'UTR, synonymous, missense (non-synonymous), and loss-of-function (LoF), which includes stop-gain and stop-loss mutations. Non-synonymous, LoF and UTR SNPs were excluded from the dataset. Following this, intergenic regions in the UCSC genome browser conservation 124-way track (insects) (https://genome.ucsc.edu/cgi-bin/hgTrackUi?db=dm6&g=cons124way) with phastCons scores ≥ 0.80 (Zheng & Zhao 2022)

were also removed (https://genome.ucsc.edu/cgi-bin/hgTrackUi?hgsid=2362308529_vdHqtNjHfKu9bHbkfr0aKlX5a2he&g=cons124way&hgTracksConfigPage=configure). After applying all filters, 1,365,568 SNPs remained in the final dataset.

Genetic map usage

We used the average recombination rate (c) of 100-kb genomic windows reported in the *D. melanogaster* genetic map for autosomes obtained by Comeron et al. (2012). Since this map represents genetic distances in centimorgans (cM) per megabase (Mb) per female meiosis, and given that Drosophila males do not undergo recombination, we halved these recombination rates. In addition, since Comeron et al.´s (2012) genetic map refers to the dm5 version, we first converted its coordinates from dm5 to dm6 using the Flybase Coordinates Converter tool (Gramates et al., 2022). Called SNPs were grouped in 100-kb windows, and those windows for which the recombination rate was not reported in Comeron et al.´s (2012) map were discarded, such that a total number of 1,356,231 SNPs in 965 windows of 100-kb were available for analysis. In particular, 395,115 SNPs in chromosome arm 2L (230 windows), 288,678 SNPs in chromosome arm 2R (211 windows), 341,012 SNPs in chromosome arm 3L (245 windows) and 331,426 SNPs in chromosome arm 3R (279 windows). Nucleotide diversity (Nei & Tajima, 1981) in the sampled individuals was obtained with VCFtools (Danecek et al., 2011) for each 100-kb window ($\bar{\pi}_{\text{window}}$). Linkage disequilibrium statistic r^2 between consecutive SNPs was obtained using PLINK (Purcell et al., 2007).

Estimation of effective population size (N_e) from linkage disequilibrium between SNPs using the software GONE

A previous estimate of the effective size (N_e) of the laboratory population in the most recent generations was obtained using a subset of 17 males, being of the order of 1,000 individuals (Novo et al., 2023b). In the present study, a more comprehensive estimation of historical N_e (going back 300 generation in the past) was obtained with the software GONE (Santiago et al., 2020; available at https://github.com/esrud/GONE) using the whole set of 51 individuals. We used a set of SNPs filtering out those with a high linkage disequilibrium ($r^2 > 0.2$) using the command *--indep-pairwise 100 20 0.20* of PLINK1.9 (Purcell et al., 2007), to obtain a total of 62,147 SNPs. For an accurate estimation of historical N_e, a precise genetic map is required. As

explained in the previous section, the genetic distances were obtained from the *D. melanogaster* genetic map (Comeron et al., 2012), corrected for the lack of recombination in males (Novo et al., 2023b). The estimation by GONE assumed the default options of the software: unknown phase, Haldane´s correction for genetic distances, no minor allele frequency pruning, use of all SNPs including those with missing data, and windows with a maximum value of recombination frequency of 0.05.

Estimation of effective population size (N_e) from the spectrum of allele frequencies with the software StairwayPlot2

An estimation of historical N_e was also obtained with the software StairwayPlot2 (Liu & Fu, 2020; available at https://github.com/xiaoming-liu/stairway-plot-v2), from the allele frequency spectrum of both variant and invariant sites sequenced in the 51 samples. Starting from the initial VCF file containing all detected SNPs, and considering all sequenced invariant positions, we computed the counts and folded frequencies of these sites, resulting in the folded Site Frequency Spectrum (fSFS). The fSFS was calculated separately for total, silent, synonymous, and nonsynonymous sites.

To obtain these spectra, we used a custom pipeline based on the mstatspop software (https://github.com/CRAGENOMICA/mstatspop) to generate the fSFS for each chromosome. The pipeline first converts the VCF file to transposed FASTA (TFA) format using gVCF2TFasta (https://github.com/sramosonsins/gVCF2tFasta). Prior to running mstatspop, silent and synonymous sites were identified following the method of Nei & Gojobori (1986) using the software fastaconvtr (https://github.com/CRAGENOMICA/fastaconvtr).

The genome-wide fSFS was obtained by summing the chromosome-specific fSFS using an R script. Chromosome 2L was excluded from genome-wide analyses because it contains large inverted regions that distort the fSFS. The fSFS was plotted for each chromosome and for the whole genome (hereafter always excluding chromosome 2L). Estimates of genomic variability were also obtained for total, silent, synonymous, and nonsynonymous sites.

Genome-wide fSFS derived from silent (74,577,602) and synonymous (3,316,854) sites were used as input for StairwayPlot2 to infer demographic history, as these site categories are

expected to evolve largely neutrally. We assumed a mutation rate of $u = 3 \times 10^{-9}$ mutations per site per generation (Wang et al., 2023) and 20 generations per year to estimate N_e through time.

Computer simulations

We used the SLiM4 software (Haller & Messer, 2023) to carry out forward-in-time simulations of a panmictic population of $N = 10{,}000$ diploid individuals for up to 50,000 discrete generations under the action of mutation, recombination, selection and drift. This ancestral effective size is justified by the estimated historical N_e obtained from the empirical data by the software GONE (shown below). Where noted, we carried out additional simulations considering an ancestral population size ten times larger ($N = 100{,}000$ individuals). In order to emulate the capture from nature and maintenance in the laboratory of the experimental Drosophila population at its estimated effective population size, at generation 49,800 the ancestral population was reduced in size to 1,000 individuals (as deduced from GONE estimates of recent N_e) and divided into 32 subpopulations of 32 individuals each that were simulated for 200 additional generations. During these last 200 generations of the simulations, a circular migration of 50% of the individuals between the subpopulations was established, mimicking the circular mixing between the 32 bottles carried out in the laboratory. In the last generation, 1 or 2 individuals from each small subpopulation were sampled (like in the experimental design), so that the genomes of 51 individuals were analysed, corresponding to the 51 flies sequenced to obtain the empirical data.

We carried out simulations for each of the four autosomal arms of *D. melanogaster* separately (2L, 2R, 3L and 3R), using Comeron et al.'s (2012) genetic map and the same corresponding adjacent 100-kb windows as for the empirical data. To closely mimic the genomic architecture of the chromosome arms, we differentiated genic (about 40% of the autosomal genome) and non-genic regions along the simulated sequences. The positions of genes were extracted from the dm5 annotated sequence of each arm available in GenBank, accession numbers AE014134.5 (chromosome arm 2L), AE013599.4 (2R), AE014296.4 (3L) and AE014297.2 (3R). Gene conversion (GC) was assumed to occur at a rate of 2×10^{-8} per nucleotide per generation, randomly distributed across the genome with tract lengths of 441 bp, following the results of Miller et al. (2016).

The parameters considered for the standard model M1 are described first. In each simulation, mutations were assumed to occur at a rate higher than typical empirical estimates, using 1.6×10^{-8} per nucleotide per generation to account for a realistic overall mutation rate. This rate enabled us to simulate the intended number of deleterious mutations, and a sufficiently large number of neutral SNPs for analysis. Table 1 shows the mutation rates, and effects and dominance of mutations for the different models investigated. Deleterious mutations (slightly or strongly deleterious) were assumed to occur in genic regions, in a 2/3 proportion, whereas the remainder 1/3 were assumed to be neutral. For each mutation with fitness effect, fitness values of 1, $1 + sh$, and $1 + s$ were assumed for the wild-type homozygote, the heterozygote, and the mutant homozygote, respectively. The fitness of each individual was assumed to be multiplicative across loci, as usually assumed for fitness (Caballero, 2020, p. 161).

Partially recessive deleterious mutations in genic regions were assumed to follow a main mutational model shown to explain the changes in inbreeding load occurred in the laboratory population (Pérez-Pereira et al., 2021), which justifies its application in the present study. Absolute values for the mutational selection coefficients were obtained from a gamma distribution with shape parameter $\beta = 0.33$ and were assigned negative sign. The mean effect of mutations was $\bar{s} = -0.2$. The dominance coefficient h of mutations was obtained from a uniform distribution between 0 and e^{ks} (Caballero & Keightley, 1994) when $s \geq -0.42$, where k is a constant to obtain a mean dominance coefficient of $\bar{h} = 0.283$. For values of $s < -0.42$, which would give values of $h < 0.04$ under the above model, h was obtained from a uniform distribution between 0 and 0.04. The above simulated mutational model itself generates lethal mutations at a rate 0.002 per haploid genome and generation, as sampled s values lower than –1 were assigned a value of $s = -1$. However, additional lethal mutations with $s = -1$ and $h = 0.02$ were also added at a rate 0.003 per haploid genome and generation. The joint distribution of s and h values of partially recessive and lethal mutations considered in the simulations is shown in Figure S1 in the Supplemental Material.

The haploid deleterious mutation rate resulting from the model ($U_{del} \approx 0.05$) and the average selection coefficient ($\bar{s} = -0.2$) are concordant with the estimates obtained from mutation-accumulation experiments for a range of higher eukaryotic species reviewed by Halligan & Keightley (2009), with a median mutation rate of 0.04, and a mean of deleterious

homozygous effect on fitness traits of –0.22. The assumed average dominance coefficient is supported by the range of estimates between 0.2 and 0.3 obtained in different studies (Crow & Simmons, 1983; García-Dorado & Caballero, 2000; Caballero, 2006; 2020, p. 158; Agrawal & Whitlock, 2011; Manna et al., 2011), and the distribution of h values assumed implies lower values for strongly deleterious mutations than for milder ones, as repeatedly observed (Mukai et al., 1972; Simmons & Crow, 1977; Caballero, 2006; Agrawal & Whitlock, 2011; Huber et al., 2018).

Because the above deleterious mutational parameters are based on mutation-accumulation experiments, which are unable to detect deleterious mutations of very small effect (say, $s > -5 \times 10^{-4}$; García-Dorado et al., 2004), slightly deleterious additive mutations of effect $s_{sdel} = -0.0001$ (for simulations with ancestral $N = 10^4$ individuals) and $s_{sdel} = -0.00001$ (for simulations with ancestral $N = 10^5$ individuals) were also added in genic regions at a rate of $U_{sdel} = 0.05$ mutations per haploid genome and generation. This type of mutations was also added in non-genic regions at a rate $U_{sdel} = 0.0125$ (5% of all mutations in these regions).

Considering as a reference the model M1 described above, we now explain the other models of Table 1. The model M1S is identical to M1 but includes also advantageous (from now on adaptive) alleles in order to incorporate the possibility of adaptation to captivity (Orozco-terWengel et al., 2012). Because the foundation of the laboratory population from the wild was 200 generations in the past, we then assumed that, after arrival to the lab, a proportion 0.003 of neutral mutations became advantageous for adaptation to lab conditions. This implies a haploid genome rate of adaptive mutations of about $U_{adap} = 0.0009$ per generation. The proportion 0.003 is obtained from the observed proportion of SNPs assumed to be under adaptation to captivity by Orozco-terWengel et al. (2012). We assumed that these adaptive mutations had additive gene action and a selection coefficient of $s = 0.05$, which is the largest estimated effect observed by Sattath et al. (2011).

We also considered alternative mutational models (see Table 1) involving a larger effect of slightly deleterious mutations ($s_{sdel} = -0.0005$) (models M2 and M2S), also a higher rate of slightly deleterious mutations (model M3), and an additional higher rate of deleterious mutations (model M4). Models were also considered where all types of mutations were additive (ADD) or fully recessive (REC). Finally, a model was considered were all mutations were neutral (NEU).

The results of the above simulation models were contrasted with those obtained empirically in order to ascertain which of them explains better the observed data.

Overdominant mutations were obtained by assuming a positive selection coefficient ($s > 0$) and $h = 1.5$ and were assigned only to genic regions. Selection coefficients were obtained from a gamma distribution with shape parameter $\beta = 0.66$ and mean effect $\bar{s} = 0.026$. These parameters were obtained by fitting a gamma distribution to the empirical selection coefficients of overdominant mutations with values lower than 0.1 reported by Thurman & Barrett (2016) (Figure S2 in the Supplemental Material). We considered models including only deleterious mutations (M1, M2, M3, M4), other including also adaptive mutations (M1S, M2S, ADD, REC), and one model (M1S) where overdominant mutations were also added at increasingly larger rates from $U_o = 0.5 \times 10^{-7}$ to 8×10^{-7} per haploid genome and generation. These rates generated a total number of genomic overdominant segregating loci in the last generation ranging from about 3 to almost 50. For simulations with ancestral $N = 10^5$, the rate of overdominant mutations was reduced by a factor of 10 in order to obtain the same approximate number of genomic overdominant segregating loci as for the simulations with $N = 10^4$. Ten independent simulations of each of the above scenarios were run for each of the four chromosome arms separately in the case of simulations with $N = 10^4$. Three replicates were run instead in the case of simulations with $N = 10^5$, given the high computer load. The mean numbers of segregating neutral (n_{neu}), slightly deleterious (n_{sdel}), deleterious (n_{del}), lethal (n_{let}), adaptive (n_{adap}) and overdominant (n_o) mutations at the last simulated generation were counted, and their mean frequencies (q) were calculated.

Additive variance (V_A), dominance variance (V_D), and inbreeding load (B; Morton et al., 1956) were calculated as $V_A = \Sigma 2\alpha^2 pq$, $V_D = \Sigma(2dpq)^2$, and $B = \Sigma 2dpq$, where the summation is for all segregating loci, p and q are the frequencies of the wild-type and mutant alleles, respectively, α is the average effect of an allelic substitution, and d is the difference between the heterozygote and the mid homozygous values. For slightly deleterious, deleterious, and lethal mutations, $d = s(h - 1/2)$, and $\alpha = sh - 2dq$ (see, e.g., Caballero, 2020, p. 180). For overdominant loci, the simulated model $(1, 1 + sh, 1 + s)$ was scaled to the classical one $(1 - s_A, 1, 1 - s_a)$ by dividing the genotype fitness values by that of the heterozygote, so that $s_A = sh / (1 + sh)$ and $s_a = s(1 + h) / (1 + sh)$, $d = (s_A + s_a) / 2$ and $\alpha = qs_a - ps_A$. The fractions of V_A, V_D and B attributable to

segregating overdominant loci were also obtained as for the other types of loci. The total values of V_A, V_D and B were obtained as the sum of values from all types of segregating selective mutations. As for the empirical data, the linkage disequilibrium statistic r^2 between consecutive neutral SNPs was computed using PLINK (Purcell et al., 2007). Nucleotide diversities (π) were obtained with VCFtools (Danecek et al., 2011) to calculate each 100-kb window average considering only neutral SNPs. To allow comparisons with the empirical values, each mean value of π was scaled by the ratio between the total number of SNPs per arm in the empirical data and in the simulations. The results of simulations from the four chromosome arms for each overdominant mutation rate (U_o) were averaged, so that ten replicates considering the complete autosomal genome were available for obtaining confidence intervals of estimates.

Because the different forms of selection (background selection, selective sweeps and balancing selection) have an impact on neutral genetic variation, particularly in regions of low recombination, we focused on the relationship between genomic diversity and recombination frequency. Thus, we examined the relationship between the mean nucleotide diversity (π) and the mean recombination rate (c) of the 100-kb windows for both the empirical and simulated data, combining the four chromosome arms. The relationship between π and c values of all genomic windows for empirical and simulated results was fitted using a rational function of the type $\pi = [(a \times c) + b] / (c + d)$, where a is the asymptote of the fitted curve and b/d is the intercept in the ordinate. This was done in R as: model <- nls(pi_vec ~ (a * c_vec + b) / (c_vec + d), start = list(a = 0.006, b = 0.002, d = 1)), where pi_vec is the vector of π values and c_vec the vector of c values for the genomic windows. For the simulation results, the curve was fitted to the average values over simulation replicates. We compared the predicted curves of the different models with the empirical curve by calculating their RMSE and also by an AIC test, also using R. We also contrasted the average nucleotide diversity of the entire autosomal genome (π) of empirical and simulated data as well as the average nucleotide diversity in genomic regions with recombination rate lower than 0.25 centimorgans (cM) per megabase (Mb) ($\pi_{c<0.25}$) using a Kolmogorov-Smirnov test. Ninety-five per cent confidence intervals for simulation results were also calculated to contrast simulation and empirical results. Confidence limits for π and linkage disequilibrium (r^2) values for empirical data were obtained by bootstrapping across window values, with ten thousand samplings of windows with replacement using a custom C programme.

Results

Estimation of effective population size across generations

The results from GONE, shown in Figure 1A, indicate that the ancestral population (the wild population of origin) had an approximate N_e of 10,000 individuals, which suddenly dropped to about 1,000 individuals at the time of capture (208 generations back, shown by the blue vertical dotted line), which then was held approximately constant over the whole period of 208 generations, except by a drop in the last 25 generations. This final drop is an expected artefact due to population structure (Santiago et al., 2020; Novo et al., 2023a) because the population was not fully panmictic, but maintained in bottles with circular mixing. Computer simulations confirmed this effect (Supplementary Figure S3). A value of $N_e \approx 1{,}000$ individuals in relation to a total number of $N \approx 2{,}800$ individuals (horizontal green dotted line) implies a ratio $N_e / N = 0.36$, which is in agreement with typical estimates of captive Drosophila populations (Frankham, 2007).

The estimates using the software Stairway Plot2 (Figure 1B) show an ancestral N_e higher than that obtained by GONE (of the order of 300,000 individuals) and a continuous decline over the last 300 generations, and particularly in the last 50, down to values below 1,000 (silent sites) or about 5,000 (synonymous sites) individuals. Estimates from around 20 generations ago (about one year back) were of the order of 10,000 individuals, and estimates around 100 generations back (about 5 years back) were of the order of 70,000 individuals, which is clearly incorrect, as the entire population was maintained at a total of about 2,800 individuals for a period of 208 generations. Thus, the estimations from Stairway Plot2 must be considered overestimations, at least in the most recent period.

Alternative indirect estimates of ancestral N_e can also be obtained from the genetic diversity observed in the sample. The nucleotide diversity (π) per nucleotide in silent positions was estimated from the fSFS as 0.0036 (excluding 2L). Considering that $\theta = 4N_e u$, a rough average estimation may be obtained as $N_e = \theta / (4u)$, i.e. $N_e(\pi) = 0.0036 \;/\; (4 \times 3\text{e}{-9}) = 300{,}000$, in agreement with the ancestral estimate of N_e from Stairway Plot2.

Impact of overdominance on nucleotide diversity

Simulations initially assumed the demographic history inferred by GONE estimations (Fig. 1A), with an ancestral $N_e = 10^4$ and a recent one of $N_e = 10^3$. Figure 2 shows the relationship between the mean nucleotide diversity for each 100-kb window (π) and the mean recombination rate (c) of that window for the empirical data (Fig. 2A) and some of the different simulated models presented in Table 1, and for models with increasing rates of overdominant mutations. The figures also show the rational function fitted to the data (for the recessive model – panel C – the function could not be fitted because of its inverted shape, and a polynomial regression is shown instead). These functions are also shown in Figure 3 for a better comparison of the different models.

For the empirical data, the lower the recombination rate, the lower the nucleotide diversity, as expected under purifying selection, resulting in an increase of the function as the recombination rate (c) increases, to reach an asymptotic plateau for high c values. First, we compared the empirical data with the models assuming no overdominant mutations. A similar function shape was obtained with all the different models (Figure 3A) except with the neutral (NEU) model (Fig. 3D and Fig. 3A) and the fully recessive (REC) model (Fig. 3C). A comparison of the fit between the function for different models and that from the empirical data is shown in the upper part of Table 2. The lowest RMSE corresponds to the model M1S and the largest to the neutral model. Accordingly, the lowest and highest AIC values correspond to these same models. The Kolmogorov-Smirnov (K-S) test comparing the π values between the empirical and simulation models for all genomic windows and for those windows with recombination rate $c < 0.25$ (Table 2), also shows that the lowest p-value is obtained for the M1S model. Therefore, the model M1S, which included adaptive mutations, is the closest to the empirical data among the different models investigated. We thus considered this as the base model, to which overdominant mutations were added. Some of the models with overdominance are presented in Figure 2 (panels F-I) for increasing rates of overdominant mutations. The middle part of Table 2 compares the model M1S and the overdominant models with the empirical data. All results suggest that the M1S model explains better the empirical data than any model assuming overdominant mutations, the second column showing the average number of overdominant mutations segregating in the genome for each of the models. The comparison

between the rational function fitted to the empirical data, the simulated data with model M1S (no overdominance) and some of the overdominant models (M1S + overdominant mutations) is shown in Figure 3B. Overdominance clearly increases the intercept of the function with the ordinate (see also Figure 2) by increasing the π values of windows with low recombination rate.

Results assuming an ancestral population size of 10^5 individuals rather than of 10^4 individuals confirmed the previous results. Figure 4 shows the relationship between the mean nucleotide diversity and the mean recombination rate, and the rational functions fitted, analogous to Figure 2, for simulation models assuming or not overdominance. The corresponding statistical tests are shown in the lowest part of Table 2. The model assuming no overdominance fits generally better to the empirical data than the models assuming overdominance, supporting the previous results with an ancestral population size of 10^4 individuals. Interestingly, the fit to empirical data of simulations assuming population size 10^5 was slightly worse than that assuming population size 10^4, as suggested by the higher RMSE obtained with size 10^5 than with size 10^4 for the four comparable cases (Table 2). Thus, in what follows we focus on the results assuming an ancestral population size of 10^4 individuals.

The average values of π for windows with $c < 0.25$ and r^2 for the empirical data (green dots), for the model M1S (no overdominance; blue dots), and for the models with overdominance (red dots) are shown in Figure 5. While the confidence limits of M1S and the empirical data overlap in both figures, only that for the lowest overdominance model does so for r^2. The effect of overdominance is an increase in π for low recombination rates and a decrease in the linkage disequilibrium between consecutive neutral variants. In summary, none of the models with overdominant mutations, except perhaps that with a very low number of overdominant mutations in terms of linkage, were compatible with the empirical results.

Impact of overdominance on allele frequencies, genetic variance and inbreeding load

Figure 6 depicts the mean number (n) and frequency (q) of segregating neutral (*neu*), slightly deleterious (*sdel*), deleterious (*del*), lethal (*let*), adaptive (*adap*) and overdominant (o) mutations with respect to the mean number of overdominant segregating mutations (n_o) corresponding to each simulated overdominant mutation rate. Increasing overdominance led to an increase in the

number of neutral and deleterious segregating mutations, and a slight decrease in their average frequency. The average frequency of overdominant mutations (n_o) was about 0.75, as expected from the asymmetrical model of overdominance considered.

Finally, Figure 7 shows the changes in the inbreeding load (B), additive variance (V_A) and dominance variance (V_D), as the average number of segregating overdominant mutations (n_o) increased. The values of B, V_A and V_D arising from non-overdominant mutations (blue lines) were kept almost invariable regardless of the level of overdominance. As expected, the values of B, V_A and V_D when all types of mutations were considered (red lines) increased substantially with increasing overdominance due to the input of these loci.

Discussion

We have attempted to quantify the contribution of overdominant loci to genetic variation by using a combined approach of genomic analysis of empirical data and computer simulations. The objective was not to ascertain the precise genetic model explaining the variation in the population, but a model which provides a scenario as close as possible to that occurred in the experimental population, in order to investigate the impact of adding overdominant variation. By quantifying the relationship between the magnitude of nucleotide diversity across genomic regions with different recombination rates, our results show that a parsimonious model of background selection from deleterious mutations and adaptation to captivity explains the observed data better than models including overdominant loci.

A key circumstance which allows the comparison between simulation and empirical results is that the recent demography of the population is known, as the population was kept in the laboratory for more than 200 generations with an approximately constant size of 2,800 individuals. We applied the software GONE to obtain estimates of N_e during this period and further back with consistent results showing a constant N_e of about 1,000 individuals (Figure 1A) in agreement with previous estimates using a lower set of individuals (Novo et al., 2023b). GONE N_e estimates also indicate an ancestral N_e of about 10,000 individuals, which suddenly declines to N_e = 1,000 almost at the precise time of capture (Figure 1A). A new version of the software recently released (GONE2; Santiago et al. 2025) could not be applied in this case, as

this version is focused on a maximum of 150 generations back in time, shorter than the time period involved in our experiment.

The estimate of ancestral N_e with GONE contrasts with those obtained from the site frequency spectrum (SFS; Stairway Plot2) or from indirect measures from the observed genetic diversity (θ), which suggest values around 300,000 individuals. The estimates from GONE are based on linkage disequilibrium between SNPs and are more reliable for recent than for ancient estimates. In contrast, estimates from the SFS are more reliable for ancient than for recent estimates, and estimates from θ refer to the harmonic mean of estimates of N_e across the whole history of coalescent events in the species. Our main simulation results correspond to a model where the demographic history of the population is that inferred by GONE, with an ancestral N_e of 10^4 individuals, but we carried out additional simulations assuming an ancestral N_e of 10^5 individuals, and the results obtained confirmed those with the lower N_e (Figure 4 and Table 2). The model excluding overdominant mutations fitted better to the empirical results than the models including overdominance, even at a very low number of overdominant loci (Table 2). Interestingly, the results assuming an ancestral $N_e = 10^4$ fitted better (lower RMSE) than those assuming $N_e = 10^5$. Thus, even when assuming a large ancestral N_e consistent with diversity-based estimates, our analyses support the conclusion that widespread segregating overdominant loci are unlikely in this system.

The average empirical mean value of nucleotide diversity at the sampling time was 0.0036 (0.0033 excluding 2L). Because our experimental population was maintained for about 200 generations with an effective size of about 1,000 individuals, the neutral diversity should have been about 10% higher at the time of the population foundation, i.e. around 0.0040, which is within the lowest range of those found in European populations (median around 0.0048) by the meta-analysis of Kapun et al. (2021). Our simulations assuming absence of overdominance (model M1S) provided a value of 0.0040 ± 0.0001 at the time of sampling, very close to the empirical one. More importantly, the average nucleotide diversity observed in regions of low recombination ($c < 0.25$ cM/Mb) was very close for empirical (0.0019) and simulation data in the absence of overdominant mutations (0.0023 ± 0.0003). The average linkage disequilibrium between consecutive neutral SNPs ($r^2 = 0.396$) was also very similar between the empirical and simulated datasets without overdominance ($r^2 = 0.398$), but as soon as overdominance was

added, the linkage disequilibrium decreased accordingly away from the empirical value. Finally, the simulated inbreeding load obtained in the absence of overdominance (model M1S) was about 0.32, which is somewhat higher than that estimated at generation 201 by Pérez-Pereira et al. (2021) (0.151 ± 0.070) comparing the means of pupae productivity of non-inbred and inbred (full-sib progeny) flies. This difference may not be surprising because pupae productivity is not likely to encompass all components of global fitness, as intended in our simulations.

Although our results suggest that a parsimonious model of background selection and adaptation to captivity is able to explain the empirical results, and that none of the models of overdominance are compatible with the empirical data, a minor contribution from overdominant loci cannot be fully discarded given the uncertainty in the simulation parameters. The lowest overdominance mutation rates considered in our simulations ($U_o = 0.5 \times 10^{-7}$, 1×10^{-7} and 2×10^{-7}) would involve only about $n_o = 3$, 5 and 11 overdominant simulated loci segregating in the population, respectively. The proportion of these mutations in relation with the deleterious and lethal ones was about 0.6%, 1% and 2%, respectively. This number of overdominant loci may be, in fact, conservatively large, as we assumed a model of overdominance with effects within the lowest range found by Thurman & Barrett (2016) (Figure S2A in the Supplemental Material). In their meta-analysis, they found 70 out of the 3,416 (or 2%) selection coefficients examined that could be assigned to overdominant selection. However, these authors already warned about the over-interpretation of their results because of statistical biases, so that the estimates would be expected to have a large error. Thus, we conservatively considered only those effects lower than 0.1 which had a gamma-shaped distribution with mean effect 0.026 (Figure S2B in the Supplemental Material). Assuming these numbers of overdominant mutations ($n_o = 3$, 5 and 11), our simulation results suggest that they would be responsible for about 13%, 18% and 34% of the inbreeding load, respectively (Figure 7A). The impact of these overdominant mutations would also be an increase in both the additive and dominance variances, of about a 35%, 46% and 54%, respectively (Figure 7B and C). Thus, a relatively small number of overdominant loci, would account for substantial amounts of inbreeding load and genetic variation.

Pseudo-overdominance, the result of interactions between deleterious recessive mutations at closely linked loci in repulsion phase (Carr & Dudash, 2003; Charlesworth & Willis, 2009; Draghi & Whitlock, 2015), can mistakenly appear as heterozygote advantage, and it is seen as a mechanism maintaining neutral diversity, especially in low recombination regions and small

populations (Schou et al., 2017; Becher et al., 2020; Gilbert et al., 2020). Thus, pseudo-overdominance may contribute to an increased nucleotide diversity observed in genomic regions of low recombination (Abu-Awad & Waller, 2023). However, this is accounted for in our simulations. It has been theoretically shown that partially recessive deleterious mutations can result in pseudo-overdominance when $2N_es < 2.5$ if linkage is sufficiently tight (Zhao & Charlesworth, 2016). For our simulated effective population size ($N_e \approx 1{,}000$), this implies mutations with $s < -0.00125$. In our simulation model, the proportion of mutations with this effect and partially recessive gene action account for about 15% of all deleterious mutations. The simulation model including exclusively additive mutations (ADD) would be devoid of pseudo-overdominance. This model was clearly less appropriate than the partially recessive model (M1S) to explain the empirical data (Table 2), suggesting that the contribution from pseudo-overdominance is necessary to explain the experimental results. However, a fully recessive model (REC), which would imply a large amount of pseudo-overdominance, is clearly inappropriate.

In our simulations, we considered a model of deleterious mutations found to be consistent with the changes in inbreeding load observed in the population (Pérez-Pereira et al., 2021) with some modifications. Although there are other possible models to be considered, this model is also shown to explain rather well the diversity observed in the population. This model, when excluding the slightly deleterious set of mutations, implies an average heterozygote effect (sh) of mutations amounting to –0.012, which is within the range of values (–0.01 to –0.02) suggested from quantitative genetic estimates for Drosophila (Crow & Simmons, 1983; Charlesworth & Hughes, 1999; Lynch et al., 1999; Charlesworth, 2015). This model of mutations refers to a fraction of mutations of relatively large effect which can be detected in mutation-accumulation experiments (García-Dorado et al., 2004; Halligan & Keightley, 2009) and which possibly includes, not only single nucleotide mutations or small indels, but also transposable element insertions and larger indels with large effects on fitness (Charlesworth, 2015). These relatively large-effect mutations are expected to be the most relevant ones when it comes to assessing the impact of inbreeding depression and the evolution of fitness in small populations and short periods of time (e.g., Caballero & Keightley, 1998; Caballero et al., 2002; Pérez-Pereira et al., 2021). However, many deleterious mutations of smaller effect, as quantified in population genomic analyses, are not included in the model. Thus, we added a class of slightly deleterious

mutations of small effects (s = –0.0001 or –0.00001) with additive gene action. This addition implied that the global average heterozygote effect (sh) of mutations got down to –0.006 or –0.0006, closer to the value estimated from population genomics analyses (around –0.001; Charlesworth, 2015). The number of neutral and deleterious mutations increased for increasing levels of overdominance, which can be explained by the general increased diversity maintained by overdominance.

Our study has the unusual advantage that the demographic history of the population is known. This knowledge is very relevant because the impact of selection on genetic variation is well known to be highly dependent on population demography (García-Dorado, 2012; Torres et al., 2019). However, we can point out several limitations of our study. First, we considered that deleterious and overdominant mutations mainly occurred in genic regions, which account for about 40% of the genome. In non-genic ones we only considered slightly deleterious mutations. Although other deleterious and overdominant mutations might also occur in non-genic regions, we believe this approximation can be more realistic than assuming mutations with strong selective effects randomly scattered along the genome. In fact, Becher et al. (2020) fully dismissed mutation in intergenic regions in their simulations investigating the impact of associative overdominance due to partially recessive deleterious and advantageous mutations. Second, modelling advantageous mutations is hard, given the scarcity of mutational parameters for this type of mutations. We assumed a proportion of neutral mutations becoming adaptive from the observations of Orozco-terWengel et al. (2012) for adaptation to captivity, and the maximum selective coefficient observed by Sattath et al. (2011). Nevertheless, our results suggest that the inclusion of these mutations improved the explanatory model (model M1S vs M1). Third, because our empirical data refer to a laboratory population, it may occur that the conditions generating balancing selection in nature may have been absent or attenuated under laboratory conditions. However, the population was maintained for a relatively short (evolutionary speaking) period of time in the lab (around 200 generations). Thus, overdominant alleles could have been maintained for that period (even if selection is relaxed), given the large population size and the high expected segregation frequency of overdominant alleles. Nevertheless, our results cannot be extrapolated to other natural or laboratory populations, and cannot serve as a global rebuttal of overdominance variation in nature. Finally, our simulated model did not consider the possibility of chromosomal inversions segregating in the population.

This would involve regions of restrained recombination, possibly subjected to strong pseudo-overdominance. However, under this latter scenario, the footprint of balancing selection would be exacerbated in the real data with respect to simulations, making our results more conservative. All in all, the remarkable agreement between the empirical and simulation results suggest that the above limitations have a restricted impact in the study.

In conclusion, our results support that the most parsimonious model of background selection, due to partially recessive deleterious mutations, and adaptation to captivity, can explain the genetic diversity observed in our experimental data better than models including overdominance. Of course, given the limitations of the models that can be simulated, a contribution from overdominance cannot be fully dismissed as a source of genetic variation and inbreeding depression, but its contribution should be, at most, minor.

Data Availability Statement

Simulation codes and scripts are available at Github address https://github.com/armando-caballero/Overdominance-in-Drosophila. FASTQ files have been deposited in the NCBI Sequence Read Archive (SRA) database under accession numbers SAMN55326084 - SAMN55326134 (BioProject accession: PRJNA1422961).

Acknowledgments

We are grateful to Timothy Thurman and Rowan Barrett for providing the raw data used in their analysis. We thank the Associate Editor (Sally Otto), and two anonymous reviewers for useful comments. We also thank Ramón Pouso for his help in developing scripts for processing genomic data, Raquel Sampedro for laboratory technical help, and Mary Riádigos for administrative support.

Funding

We acknowledge financial support from grants PID2020-114426GB-C21 (funded by MCIN/AEI/10.13039/501100011033), Xunta de Galicia (ED431C 2024-22), Centro singular de investigación de Galicia accreditation 2024-2027 (ED431G 2023/07) and "ERDF A way of making Europe". IGC was funded by the Spanish Ministry of Universities (Margarita Salas postdoctoral fellowship, ref. RSU.UDC.MS17). Funding for open access charge: Universidade de Vigo/CISUG.

Conflict of Interest

The authors declare no conflict of interest.

References

Agrawal, A. F., & Whitlock, M. C. (2011). Inferences about the distribution of dominance drawn from yeast gene knockout data. *Genetics*, **187**, 553‑566. https://doi.org/10.1534/genetics.110.124560

Abu-Awad, D., & Waller, D. (2023). Conditions for maintaining and eroding pseudo-overdominance and its contribution to inbreeding depression. *Peer Community J.* **3**, e8. https://doi.org/10.24072/pci. evolbiol.100531

Allison, A. C. (1954). Protection afforded by sickle-cell trait against subtertian malarial infection. *British Medical Journal,* **1**, 290–294. https://doi.org/10.1136/bmj.1.4857.290

Andrés, A. M., Hubisz, M. J., Indap, A., Torgerson, D. G., Degenhardt, J. D., Boyko, A. R., Gutenkunst, R. N., White, T. J., Green, E. D., Bustamante, C. D., Clark, A. G., & Nielsen, R. (2009). Targets of balancing selection in the human genome. *Molecular Biology and Evolution,* **26**(12), 2755-64. https://doi.org/10.1093/molbev/msp190

Andrews, S. (2010). FastQC: A quality control tool for high throughput sequence data. http://www.bioinformatics.babraham.ac.uk/projects/fastqc/

Ayroles, J. F., Hughes, K. A., Rowe, K. C., Reedy, M. M., Rodriguez-Zas, S. L., Drnevich, J. M., Cáceres, C. E., & Paige, K. N. (2009). A genomewide assessment of inbreeding depression: gene number, function, and mode of action. *Conservation Biology*, **23**, 920–93. https://doi.org/10.1111/j.1523-1739.2009.01186.x

Barrett, S. C. H., & Charlesworth, D. (1991). Effects of a change in the level of inbreeding on the genetic load. *Nature,* **352**, 522–524. https://doi.org/10.1038/352522a0

Becher, H., Jackson, B. C., & Charlesworth, B. (2020). Patterns of genetic variability in genomic regions with low rates of recombination. *Current Biology*, **30**, 94–100. https://doi.org/10.1016/j.cub.2019.10.047

Begun, D. J., & Aquadro, C. F. (1992). Levels of naturally occurring DNA polymorphism correlate with recombination rates in *D. melanogaster*. *Nature,* **356**, 519–520. https://doi.org/10.1038/356519a0

Berry, A. J., Ajioka, J. W., & Kreitman, M. (1991). Lack of polymorphism on the Drosophila fourth chromosome resulting from selection. *Genetics*, *129*(4), 1111-1117.

Bersabé, D., Caballero, A., Pérez-Figueroa, A., & García-Dorado, A. (2015). On the consequences of purging and linkage on fitness and genetic diversity. *G3: Genes, Genomes, Genetics,* **6**(1), 171-181. https://doi: 10.1534/g3.115.023184

Bitarello, B. D., de Filippo, C., Teixeira, J. C., Schmidt, J. M., Kleinert, P., Meyer, D., & Andrés, A. M. (2018). Signatures of long-term balancing selection in human genomes. *Genome Biology and Evolution*, **10**(3), 939–55. https://doi.org/10.1093/gbe/evy054

Bolger, A. M., Lohse, M., & Usadel, B. (2014). Trimmomatic: a flexible trimmer for Illumina sequence data. *Bioinformatics,* **30**(15), 2114-2120. https://doi.org/10.1093/bioinformatics/btu170

Caballero, A. (2006). Analysis of the biases in the estimation of deleterious mutation parameters from natural populations at mutation-selection balance. *Genetics Research,* **88**, 177–189. https://doi.org/10.1017/S0016672307008506

Caballero, A. (2020). *Quantitative Genetics*. Cambridge, U.K.: Cambridge University Press.

Caballero, A., Cusi, E., Garcia, C., & Garcia-Dorado, A. (2002). Accumulation of deleterious mutations: additional *Drosophila melanogaster* estimates and a simulation of the effects of selection. *Evolution,* **56**, 1150–1159. https://doi. org/10. 1111/j.0014-3820.

Caballero, A., & Keightley, P. D. (1994). A pleiotropic nonadditive model of variation in quantitative traits. *Genetics*, **138**, 883–900. https://doi.org/10.1093/genetics/138.3.883

Carr, D. E., & Dudash, M. R. (2003). Recent approaches into the genetic basis of inbreeding depression in plants. *Philosophical Transactions of the Royal Society B: Biological Sciences,* **358**, 1071–1084. https://doi.org/10.1098/rstb.2003.1295

Charlesworth, B. (2015). Causes of natural variation in fitness: evidence from studies of *Drosophila* populations. *Proceedings of the National Academy of Sciences,* **112**, 1662–1669. https://doi.org/10.1073/pnas.142327511

Charlesworth, B., & Campos, J. L. (2014). The relations between recombination rate and patterns of molecular variation and evolution in *Drosophila*. *Annual Review of Genetics,* **48**, 383–403. https://doi.org/10.1146/annurev-genet-120213-092525

Charlesworth, B., & Charlesworth, D. (1999). The genetic basis of inbreeding depression. *Genetics Research*, **74**, 329–340. https://doi.org/10.1017/S0016672399004152

Charlesworth, B., & Hughes, K. A. (1999). The quantitative genetics of life history traits. In Singh, R. S., & Krimbas, C. B. (Ed.). *Evolutionary Genetics from Molecules to Morphology* (pp. 369–392). Cambridge, England: Cambridge University Press.

Charlesworth, B., & Morgan, M. T., & Charlesworth, D. (1993). The effect of deleterious mutations on neutral molecular variation. *Genetics*, **134**(4), 1289-303. https://doi.org/10.1093/genetics/134.4.1289

Charlesworth, D. (2006). Balancing selection and its effects on sequences in nearby genome regions. *PLoS Genetics,* **2**(4), e64. https://doi.org/10.1371/journal.pgen.0020064

Charlesworth, D., & Charlesworth, B. (1987). Inbreeding depression and its evolutionary consequences. *Annual Review of Ecology, Evolution, and Systematics,* **18**, 237–268. https://doi.org/10.1146/annurev.es.18.110187.001321

Charlesworth, D., & Willis, J. (2009). The genetics of inbreeding depression. *Nature Reviews Genetics,* **10**, 783–796. https://doi.org/10.1038/nrg2664

Comeron, J. M. (2014). Background selection as baseline for nucleotide variation across the Drosophila genome. *PLoS Genetics,* **10**, e1004434. https://doi.org/10.1371/journal.pgen.1004434

Comeron, J. M. (2017). Background selection as null hypothesis in population genomics: insights and challenges from Drosophila studies. *Philosophical Transactions of the Royal Society B: Biological Sciences,* **372**, 20160471. http://doi.org/10.1098/rstb.2016.0471

Comeron, J. M., Ratnappan, R., & Bailin, S. (2012). The many landscapes of recombination in *Drosophila melanogaster*. *PLoS Genetics,* **8**(10), e1002905. https://doi.org/10.1371/journal.pgen.1002905

Corbett, S., Courtiol, A., Lummaa, V., Moorad, J., & Stearns, S. (2018). The transition to modernity and chronic disease: mismatch and natural selection. *Nature Reviews Genetics,* **19**, 419–430. https://doi.org/10.1038/s41576-018-0012-3

Crnokrak, P., & Barrett, S. C. (2002). Perspective: purging the genetic load: a review of the experimental evidence. *Evolution,* **56**, 2347–2358. https://doi.org/10.1111/j.0014-3820.2002.tb00160.x

Crow, J. F. (1999). Dominance and overdominance. *Genetics and Exploitation of Heterosis in Crops*, 49-58. https://doi.org/10.2134/1999.geneticsandexploitation.c5

Crow, J. F., & Simmons, M. J. (1983). The mutation load in Drosophila. In Ashburner, M., Carson, H. L., & Thompson, J. N. (Ed.). *The Genetics and Biology of Drosophila* (pp. 1-35). London, England: Academic Press.

Cutter, A., & Payseur, B. (2013). Genomic signatures of selection at linked sites: unifying the disparity among species. *Nature Reviews Genetics,* **14**, 262–274. https://doi.org/10.1038/nrg3425

Danecek, P., Auton, A., Abecasis, G., Albers, C. A., Banks, E., DePristo, M. A., Handsaker, R. E., Lunter, G., Marth, G. T., Sherry, S. T., McVean, G., & Durbin, R. (2011). The variant call

format and VCFtools. *Bioinformatics*, **27**(15), 2156-2158. https://doi.org/10.1093/bioinformatics/btr330

Danecek, P., Bonfield, J. K., Liddle, J., Marshall, J., Ohan, V., Pollard, M. O., Whitwham, A., Keane, T., McCarthy, S. A., Davies, R. M., & Li, H. (2021). Twelve years of SAMtools and BCFtools. *Gigascience*, **10**(2), giab008. https://doi.org/10.1093/gigascience/giab008

Del Fabbro, C., Scalabrin, S., Morgante, M., & Giorgi, F. M. (2013). An extensive evaluation of read trimming effects on Illumina NGS data analysis. *PLoS One,* **8**(12), e85024. https://doi.org/10.1371/journal.pone.0085024

Draghi, J., & Whitlock, M. C. (2015). Overdominance interacts with linkage to determine the rate of adaptation to a new optimum. *Journal of Evolutionary Biology,* **28**(1), 95-104. https://doi.org/10.1111/jeb.12547

Dussex, N., Morales, H. E., Grossen, C., Dalén, L., & van Oosterhout, C. (2023). Purging and accumulation of genetic load in conservation. *Trends in Ecology & Evolution,* **38**(10), 962-969. https://doi.org/10.1016/j.tree.2023.05.008

Elyashiv, E., Sattath, S., Hu, T. T., Strutsovsky, A., McVicker, G., Andolfatto, P., Coop, G., & Sella, G. (2016). A genomic map of the effects of linked selection in Drosophila. *PLoS Genetics,* **12**(8), e10061. https://doi.org/10.1371/journal.pgen.1006130

Fernández, B., García-Dorado, A., & Caballero, A. (2005). The effect of antagonistic pleiotropy on the estimation of the average coefficient of dominance of deleterious mutations. *Genetics*, **171**(4), 2097-112. https://doi:10.1534/genetics.105.044750

Fijarczyk, A., & Babik, W. (2015). Detecting balancing selection in genomes: limits and prospects. *Molecular Ecology,* **24**(14), 3529-3545. https://doi.org/10.1111/mec.13226

Frankham, R. (2007). Effective population size/adult population size ratios in wildlife: a review. *Genet Res.*, **89(5-6)**, 491-503. https://doi.org/10.1017/S0016672308009695.

Frydenberg, O. (1963). Population studies of a lethal mutant in *Drosophila melanogaster*. *Hereditas*, **50**, 89–116. https://doi.org/10.1111/j.1601-5223.1963.tb01896.x

Gao, Z., Przeworski, M., & Sella, G. (2015). Footprints of ancient balanced polymorphisms in genetic variation: Data from closely related species. *Evolution*, **69**, 431–466. https://doi.org/10.1111/evo.12567

García-Dorado, A. (1986). The effect of niche preference on polymorphism protection in a heterogeneous environment. *Evolution,* **40**(5), 936-945. https://doi.org/10.1111/j.1558-5646.1986.tb00562.x

García-Dorado, A. (2012). Understanding and predicting the fitness decline of shrunk populations: inbreeding, purging, mutation, and standard selection. *Genetics*, **190**(4), 1461–1476. https://doi.org/10.1534/genetics.111.135541

García-Dorado, A., & Caballero, A. (2000). On the average coefficient of dominance of deleterious spontaneous mutations. *Genetics*, **155**(4), 1991–2001. https://doi.org/10.1093/genetics/155.4.1991

García-Dorado, A., López-Fanjul, C., & Caballero, A. (2004). Rates and effects of deleterious mutations and their evolutionary consequences. In Moya, A., & Font, E. (Ed.). *Evolution: From molecules to ecosystems* (pp. 20-32). Oxford, England: Oxford University Press.

Gemmell, N. J., & Slate, J. (2006). Heterozygote advantage for fecundity. *PLoS ONE*, **1**, e125. https://doi.org/10.1371/journal.pone.0000125

Gilbert, K. J., Pouyet, F., Excoffier, L., & Peischl, S. (2020). Transition from background selection to associative overdominance promotes diversity in regions of low recombination. *Current Biology,* **30**(1), 101-107. https://doi.org/10.1016/j.cub.2019.11.063

González-Castellano, I., Ordás, P., & Caballero, A. (2025a). Estimation of inbreeding depression from overdominant loci using molecular markers. *Evolutionary Applications*, **18**(3), e70085. doi: 10.1111/eva.70085.

González-Castellano, I., García-Dorado, A., & Caballero, A. (2025b). Inbreeding load infinite populations from dominant and overdominant mutations. *Proceedings of the Royal Society B*, **292**: 20250845. https://doi.org/10.1098/rspb.2025.0845

Gramates, L. S., Agapite, J., Attrill, H., Calvi, B. R., Crosby, M. A., dos Santos, G., Goodman, J. L., Goutte-Gattat, D., Jenkins, V. K., Kaufman, T., Larkin, A., Matthews, B. B., Millburn, G., Strelets, V. B., & the FlyBase consortium. (2022). FlyBase: A guided tour of highlighted features. *Genetics*, **220**(4), iyac035. https://doi.org/10.1093/genetics/iyac035

Haller, B. C., & Messer, P. W. (2023). SLiM 4: Multispecies eco-evolutionary modeling. *American Naturalist*, **201**(5), E127-E139. doi: 10.1086/723601.

Halligan, D. L., & Keightley, P. D. (2009). Spontaneous mutation accumulation studies in evolutionary genetics. *Annual Review of Ecology, Evolution, and Systematics*, **40**, 151-172. https://doi.org/10.1146/annurev.ecolsys.39.110707.173437

Hasselgren, M., & Norén, K. (2019). Inbreeding in natural mammal populations: Historical perspectives and future challenges. *Mammal Review*, **49**(4), 369-383. https://doi.org/10.1111/mam.12169

Hedrick, P. W. (2012). What is the evidence for heterozygote advantage selection? *Trends in Ecology & Evolution*, **27**, 698–704. https://doi.org/10.1016/j.tree.2012.08.012

Hedrick, P. W., & García-Dorado, A. (2016). Understanding inbreeding depression, purging, and genetic rescue. *Trends in Ecology & Evolution*, **31**, 940–952. https://doi.org/10.1016/j.tree.2016.09.005

Huber, C. D., Durvasula, A., Hancock, A. M., & Lohmueller, K. E. (2018). Gene expression drives the evolution of dominance. *Nature Communications,* **9**(1), 2750. https://doi.org/10.1038/s41467-018-05281-7

Hudson, R. R. (1990). Gene genealogies and the coalescent process. *Oxford Surveys in Evolutionary Biology*, *7*(1), 44.

Hudson, R. R., Kreitman, M., & Aguadé, M. (1987). A test of neutral molecular evolution based on nucleotide data. *Genetics,* **116**(1), 153-159. https://doi.org/10.1093/genetics/116.1.153

Johnston, S. E., Gratten, J., Berenos, C., Pilkington, J. G., Clutton-Brock, T. H., Pemberton, J. M., & Slate, J. (2013). Life history trade-offs at a single locus maintain sexually selected genetic variation. *Nature*, **502**(7469), 93-95. https://doi.org/10.1038/nature12489

Kapun M, Nunez JC, Bogaerts-Márquez M, Murga-Moreno J, Paris M, Outten J, Coronado-Zamora M, Tern C, Rota-Stabelli O, García-Guerreiro MP, Casillas, S., Orengo, D. J., Puerma, E., Kankare, M., Ometto, L., Loeschcke, V., Onder. B. S., Abbott J. K., Schaeffer S. W., … Bergland, A. O. (2021). Drosophila evolution over space and time (DEST): a new population genomics resource. *Molecular Biology and Evolution,* **38**(12), 5782-5805. https://doi.org/10.1093/molbev/msab259

Keller, L. F., & Waller, D. M. (2002). Inbreeding effects in wild populations. *Trends in Ecology & Evolution,* **17**(5), 230-241. https://doi.org/10.1016/S0169-5347(02)02489-8

Kimura, M., & Ohta, T. (1971). *Theoretical topics in population genetics*. Princeton (NJ): Princeton University Press.

Lande, R. (1976). Natural selection and random genetic drift in phenotypic evolution. *Evolution,* **30**, 314–334. https://doi.org/10.2307/2407703

Lemaître, J. F., Berger, V., Bonenfant, C., Douhard, M., Gamelon, M., Plard, F., & Gaillard, J. M. (2015). Early-late life trade-offs and the evolution of ageing in the wild. *Proceedings of the Royal Society B: Biological Sciences,* **282**(1806), 20150209. https://doi.org/10.1098/rspb.2015.0209

Li, H. (2013). Aligning sequence reads, clone sequences and assembly contigs with BWA-MEM. *arXiv*, 1303.3997. https://doi.org/10.48550/arXiv.1303.3997

Liu, X., Fu, YX. (2020). Stairway Plot 2: demographic history inference with folded SNP frequency spectra. *Genome Biology*, **21**, 280. https://doi.org/10.1186/s13059-020-02196-9

López-Cortegano, E., Vilas, A., Caballero, A., & García-Dorado, A. (2016). Estimation of genetic purging under competitive conditions. *Evolution*, **70**(8), 1856–1870. https://doi.org/10.1111/evo.12983

Lynch, M., Blanchard, J., Houle, D., Kibota, T., Schultz, S., Vassilieva, L., & Willis, J. (1999). Perspective: Spontaneous deleterious mutation. *Evolution,* **53**(3), 645-663. https://doi.org/10.1111/j.1558-5646.1999.tb05361.x

Manna, F., Martin, G., & Lenormand, T. (2011). Fitness landscapes: An alternative theory for the dominance of mutation. *Genetics,* **189**(3), 923–937. https://doi.org/10.1534/genetics.111.132944

Maynard-Smith, J., & Haigh, J. (1974). The hitchhiking effect of a favorable gene. *Genetics Research*, **23**, 23-35. https://doi.org/10.1017/S0016672300014634

Miller, D.E., Smith, C.B., Kazemi, N.Y., Cockrell, A.J., Arvanitakis, A.V., Blumenstiel, J.P., Jaspersen, S.L., & Hawley, R.S. (2016). Whole-Genome Analysis of individual meiotic events in *Drosophila melanogaster* reveals that noncrossover gene conversions are insensitive to interference and the centromere effect. *Genetics*, **203(1)**, 159-71. https://doi.org/10.1534/genetics.115.186486.

Minias, P., & Vinkler, M. (2022). Selection balancing at innate immune genes: adaptive polymorphism maintenance in toll-like receptors. *Molecular Biology and Evolution,* **39**(5), msac102. https://doi.org/10.1093/molbev/msac102

Morton, N. E., Crow, J. F., & Muller, H. J. (1956). An estimate of the mutational damage in man from data on consanguineous marriages. *Proceedings of the National Academy of Sciences,* **42**, 855–863. https://doi.org/10.1073/pnas.42.11.855

Mukai, T. (1988). Genotype-environment interaction in relation to the maintenance of genetic variability in populations of *Drosophila melanogaster*. In Weir, B. S., Eisen, E. J., Goodman, M. M. & Namkoong, G. (Ed.). Proceedings of the second international conference on quantitative genetics (pp. 21–31). Sunderland (MA): Sinauer Press.

Mukai, T., Chigusa, S. I., Mettler, L. E., & Crow, J. F. (1972). Mutation rate and dominance of genes affecting viability in *Drosophila melanogaster*. *Genetics,* **72**, 333‑355. https://doi.org/10.1093/genetics/72.2.335

Nei, M., and T. Gojobori. (1986). Simple methods for estimating the number of synonymous and nonsynonymous nucleotide substitutions. *Mol. Biol. Evol.* **3**, 418–426. https://doi.org/10.1093/oxfordjournals.molbev.a040410

Nei, M., & Tajima, F. (1981). DNA polymorphism detectable by restriction endonucleases. *Genetics,* **97**(1), 145-163. https://doi.org/10.1093/genetics/97.1.145

Nielsen, R. (2005). Molecular signatures of natural selection. *Annual Review of Genetics,* 39, 197-218. https://doi.org/10.1146/annurev.genet.39.073003.112420

Novo I, Ordás P, Moraga N, Santiago E, Quesada H, & Caballero, A. (2023a). Impact of population structure in the estimation of recent historical effective population size by the software GONE. *Genetics Selection Evolution* **55**(1), 86 https://doi.org/10.1186/s12711-023-00859-2

Novo, I., Pérez-Pereira, N., Santiago, E., Quesada, H., & Caballero, A. (2023b). An empirical test of the estimation of historical effective population size using *Drosophila melanogaster. Molecular Ecology Resources*, **23**(7), 632-1640. https://doi.org/10.1111/1755-0998.13837

Ohta, T. (1971). Associative overdominance cause by linked detrimental mutations. *Genetics Research,* **18**, 277–286. https://doi.org/10.1017/S0016672300012684

Okonechnikov, K., Conesa, A., & García-Alcalde, F. (2016). Qualimap 2: advanced multi-sample quality control for high-throughput sequencing data. *Bioinformatics,* **32**(2), 292-294. https://doi.org/10.1093/bioinformatics/btv566

Orozco-terWengel, P., Kapun, M., Nolte, V., Kofler, R., Flatt, T., & Schlötterer, C. (2012). Adaptation of Drosophila to a novel laboratory environment reveals temporally heterogeneous trajectories of selected alleles. *Molecular Ecology* **21(20)**, 4931-41. https://doi.org/10.1111/j.1365-294X.2012.05673.x

Paige, K. N. (2010). The functional genomics of inbreeding depression: a new approach to an old problem. *BioScience,* **60**(4), 267-277. https://doi.org/10.1525/bio.2010.60.4.5

Pamilo, P., & Pálsson, S. (1998). Associative overdominance, heterozygosity and fitness. *Heredity*, **81**(4), 381-389. https://doi.org/10.1046/j.1365-2540.1998.00395.x

Partridge, G. G. (1979). Relative fitness of genotypes in a population of *Rattus norvegicus* polymorphic for warfarin resistance. *Heredity*, **43**, 239–246. https://doi.org/10.1038/hdy.1979.79

Pérez-Pereira, N., Pouso, R., Rus, A., Vilas, A., López-Cortegano, E., García-Dorado, A., Quesada, H., & Caballero, A. (2021). Long-term exhaustion of the inbreeding load in

Drosophila melanogaster. *Heredity,* **127**, 373–383. https://doi.org/10.1038/s41437-021-00464-3

Peters, A. D., Halligan, D. L., Whitlock, M. C., & Keightley, P. D. (2003). Dominance and overdominance of mildly deleterious induced mutations for fitness traits in *Caenorhabditis elegans*. *Genetics,* **165**, 589-599. https://doi.org/10.1093/genetics/165.2.589

Purcell, S., Neale, B., Todd-Brown, K., Thomas, L., Ferreira, M. A. R., Bender, D., Maller, J., Sklar, P., de Bakker, P. I. W., Daly, M. J., Sham, P. C. (2007). PLINK: A tool set for whole-genome association and population-based linkage analyses. *American Journal of Human Genetics*, 81, 559–575. https://doi.org/10.1086/519795

Rodríguez, J. A., Marigorta, U. M., Hughes, D. A., Spataro, N., Bosch, E., & Navarro, A. (2017). Antagonistic pleiotropy and mutation accumulation influence human senescence and disease. *Nature Ecology & Evolution,* **1**(3), 0055. https://10.1038/s41559-016-0055.

Roff, D. A. (1997). *Evolutionary Quantitative Genetics*. New York (NY): Chapman & Hall.

Roff, D. A. (2002). Inbreeding depression: tests of the overdominance and partial dominance hypotheses. *Evolution*, **56**, 768–775. https://doi.org/10.1111/j.0014-3820.2002.tb01387.x

Rose, M. R. (1982). Antagonistic pleiotropy, dominance, and genetic variation. *Heredity*, **48**, 63–78. https://doi.org/10.1038/hdy.1982.7

Santiago, E., & Caballero, A. (1998). Effective size and polymorphism of linked neutral loci in populations under directional selection. *Genetics*, 149(4), 2105-17. https://doi.10.1093/genetics/149.4.2105.

Santiago, E., Novo, I., Pardiñas, A.F., Saura, M., Wang, J., & Caballero, A. (2020). Recent demographic history inferred by high-resolution analysis of linkage disequilibrium. *Molecular Biology and Evolution*, **37(12)**, 3642-3653. https://doi10.1093/molbev/msaa169

Santos, M. (1997). On the contribution of deleterious alleles to fitness variance in natural populations of Drosophila. *Genetics Research,* **70**(2), 105-115. https://doi.org/10.1017/S0016672397002942

Sattath, S., Elyashiv, E., Kolodny, O., Rinott, Y., & Sella, G. (2011). Pervasive adaptive protein evolution apparent in diversity patterns around amino acid substitutions in *Drosophila simulans*. *PLoS Genetics*, 10;7(2): e1001302. https://doi: 10.1371/journal.pgen.1001302.

Schou, M. F., Bechsgaard, J., Muñoz, J., & Kristensen, T. N. (2018). Genome-wide regulatory deterioration impedes adaptive responses to stress in inbred populations of *Drosophila melanogaster*. *Evolution*, **72**(8), 1614–1628. https://doi.org/10.1111/evo.13497

Schou, M. F., Loeschcke, V., Bechsgaard, J., Schlotterer, C., & Kristensen, T. N. (2017). Unexpected high genetic diversity in small populations suggests maintenance by associative overdominance. *Molecular Ecology,* **26**, 6510–6523. https://doi.org/10.1111/mec.14262

Sharp, N.P., & Agrawal, A. F. (2018). An experimental test of the mutation- selection balance model for the maintenance of genetic variance in fitness components. *Proceedings of the Royal Society B: Biological Sciences*, **285**, 20181864. https://doi.org/10.1098/rspb.2018.1864

Sianta, S. A., Peischl, S., Moeller, D. A., & Brandvain, Y. (2023). The efficacy of selection may increase or decrease with selfing depending upon the recombination environment. *Evolution*, **77**(2), 394-408. https://doi.org/10.1093/evolut/qpac013

Siewert, K. M., & Voight, B. F. (2017). Detecting long-term balancing selection using allele frequency correlation. *Molecular Biology and Evolution,* **34**(11), 2996-3005. https://doi.org/10.1093/molbev/msx209

Simmons, M. J., & Crow, J. F. (1977). Mutations affecting fitness in Drosophila populations. *Annual Review of Genetics,* **11**(1), 49-78. https://doi.org/10.1146/annurev.ge.11.120177.000405

Slatkin, M. (2000). Balancing selection at closely linked, overdominant loci in a finite population. *Genetics*, **154**(3), 1367-78. https://doi.org/10.1093/genetics/154.3.1367

Soni, V., Vos, M., & Eyre-Walker, A. (2022). A new test suggests hundreds of amino acid polymorphisms in humans are subject to balancing selection. *PLoS Biol*ogy, **20**(6), e3001645. https://doi.org/10.1371/journal.pbio.3001645

Swindell, W., & Bouzat, J. (2006). Reduced inbreeding depression due to historical inbreeding in *Drosophila melanogaster*: evidence for purging. *Journal of Evolutionary Biology,* **19**, 1257–1264. https://doi.org/10.1111/j.1420-9101.2005.01074.x

Tajima, F. (1989). Statistical method for testing the neutral mutation hypothesis by DNA polymorphism. *Genetics*, **123**, 585–595. https://doi.org/10.1093/genetics/123.3.585

Thurman, T. J., & Barrett, R. D. (2016). The genetic consequences of selection in natural populations. *Molecular Ecology,* **25**, 1429–1448. https://doi.org/10.1111/mec.13559

Torres, R., Szpiech, Z. A., & Hernandez, R. D. (2019). Human demographic history has amplified the effects of background selection across the genome. *PLoS Genetics,* **14**(6), e1007387. https://doi.org/10.1371/journal.pgen.1007387. Erratum in: *PLoS Genetics,* **15**(1), e1007898. https://doi.org/10.1371/journal.pgen.1007898

Van der Auwera, G. A., & O'Connor, B. D. (2020). *Genomics in the cloud: using Docker, GATK, and WDL in Terra.* O'Reilly Media.

Waller, D. M. (2021). Addressing Darwin's dilemma: can pseudo-overdominance explain persistent inbreeding depression and load? *Evolution,* **75**, 779–793. https://doi.org/10.1111/evo.14189

Wang, K., Li, M., & Hakonarson, H. (2010). ANNOVAR: functional annotation of genetic variants from high-throughput sequencing data. *Nucleic Acids Research*, **38**, e164

Wang, B., Mojica, J. P., Perera, N., Lee, C. R., Lovell, J. T., Sharma, A., Adam, C., Lipzen, A., Barry, K., Rokhsar, D. S., Schmutz, J., & Mitchell-Olds, T. (2019). Ancient polymorphisms contribute to genome-wide variation by long-term balancing selection and divergent sorting in *Boechera stricta*. *Genome Biology*, **20**, 1-15. https://doi.org/10.1186/s13059-019-1729-9

Wang Y, McNeil P, Abdulazeez R, Pascual M, Johnston SE, Keightley PD, Obbard DJ. (2023). Variation in mutation, recombination, and transposition rates in *Drosophila*

melanogaster and *Drosophila simulans*. *Genome Res.* **33(4)**, 587–598. https://doi.org/10.1101/gr.277383.122.

Wang, K., Li, M., & Hakonarson, H. (2010). ANNOVAR: functional annotation of genetic variants from high-throughput sequencing data. *Nucleic Acids Research*, **38**, e164

Wright, S. (1931). Evolution in mendelian populations. *Genetics*, **16**, 97–159.

Yang, J., Mezmouk, S., Baumgarten, A., Buckler, E. S., Guill, K. E., McMullen, M. D., Mumm, R. H., & Ross-Ibarra, J. (2017). Incomplete dominance of deleterious alleles contributes substantially to trait variation and heterosis in maize. *PLoS Genetics,* **13**, e1007019. https://doi.org/10.1371/journal.pgen.1007019

Zhao, L., & Charlesworth, B. (2016). Resolving the conflict between associative overdominance and background selection. *Genetics,* **203**, :1315–1334. https://doi.org/10.1534/genetics.116.188912

Zheng, E.B, & Zhao, L. (2022). Protein evidence of unannotated ORFs in Drosophila reveals diversity in the evolution and properties of young proteins. *eLife*, **11**: e78772. https://doi.org/10.7554/eLife.78772

Table 1. Mutational parameters assumed in the simulations without overdominant mutations. U, s and h are the haploid genomic mutation rate, the effect or average effect of mutations in homozygotes, and the dominance coefficient or its average, respectively, for neutral (subscript *neu*), deleterious (*del*), slightly deleterious (*sdel*), lethal (*let*) and adaptive (*adap*) mutations. Model M1S was chosen to further include overdominant mutations as explained in the main text.

Model	U_{neu}	U_{del}	s_{del}	h_{del}	U_{sdel}	s_{sdel}	h_{sdel}	U_{let}	h_{let}	U_{adap}	s_{adap}	h_{adap}
M1	0.274	0.049	–0.2	0.283	0.06	–0.0001	0.5	0.003	0.02	0	0	0
M1S*	0.273	0.049	–0.2	0.283	0.06	–0.0001	0.5	0.003	0.02	0.0009	0.05	0.5
M2	0.274	0.049	–0.2	0.283	0.06	–0.0005	0.5	0.003	0.02	0	0	0
M2S	0.273	0.049	–0.2	0.283	0.06	–0.0005	0.5	0.003	0.02	0.0009	0.05	0.5
M3	0.262	0.049	–0.2	0.283	0.072	–0.0005	0.5	0.003	0.02	0	0	0
M4	0.328	0.061	–0.2	0.283	0.091	–0.0005	0.5	0.003	0.02	0	0	0
ADD	0.273	0.049	–0.2	0.5	0.06	–0.0001	0.5	0.003	0.5	0.0009	0.05	0.5
REC	0.273	0.049	–0.2	0	0.06	–0.0001	0	0.003	0	0.0009	0.05	0
NEU	0.386	0	-	-	0	-	-	0	-	0	-	-

* For simulations with ancestral $N_e = 10^5$, the same parameters were used except that $s_{sdel} = -0.00001$.

Table 2. Statistical comparison between the results obtained with the different models simulated and the empirical data. The upper part of the table compares model assuming no overdominant (OD) mutations (see Table 1) assuming an ancestral $N_e = 10^4$ individuals, while the middle part compares the best model found without overdominant mutations (M1S, in bold) with models assuming different OD mutation rates (U_o): 0.5×10^{-7} (SD005), 1×10^{-7} (SD01), 2×10^{-7} (SD02), 4×10^{-7} (SD04), 6×10^{-7} (SD06), 8×10^{-7} (SD08). The lower part of the table gives results assuming an ancestral $N_e = 10^5$ individuals. The second column (n_o) shows the average number of segregating OD mutations in the analysed simulated populations. RMSE and AIC are the Root Mean Squared Error and Akaike Information Criterion, respectively, comparing the rational function fitted to the empirical π values from genomic windows with those fitted to simulated data from different models. K-S refers to the probability value of the Kolmogorov-Smirnov test comparing the empirical π values from genomic windows with those simulated data from different models.

	n_o	RMSE	AIC	K-S (π)	K-S ($\pi_{c<0.25}$)
No OD models - Ancestral $N_e = 10^4$					
M1	0	0.000432	-14931.65	1.91E-07	0.00E+00
M1S	0	**0.000099**	**-17774.54**	**1.91E-02**	**1.04E-06**
M2	0	0.000215	-16280.39	2.18E-05	4.10E-12
M2S	0	0.000744	-13885.35	1.12E-03	1.13E-08
M3	0	0.000285	-15736.76	5.15E-07	6.16E-09
M4	0	0.000359	-15291.43	8.47E-07	3.38E-11
ADD	0	0.000367	-15246.65	4.53E-04	4.56E-13
REC	0	-	-	7.93E-13	0.00E+00
NEU	0	0.001112	-13109.60	0.00E+00	0.00E+00
No OD vs OD models - Ancestral $N_e = 10^4$					
M1S	**0**	**0.000099**	**-17774.54**	**1.91E-02**	**1.04E-06**
SD005	2.8	0.000368	-15244.14	1.42E-04	3.38E-11
SD01	5.1	0.000179	-16634.28	1.76E-06	0.00E+00
SD02	10.8	0.000172	-16712.18	1.08E-06	0.00E+00
SD04	22.3	0.000344	-15368.97	1.68E-09	0.00E+00
SD06	36.0	0.000493	-14676.43	2.21E-12	0.00E+00
SD08	47.3	0.000549	-14470.24	1.97E-13	0.00E+00
No OD vs OD models - Ancestral $N_e = 10^5$					
M1S	**0**	**0.000207**	**-16363.90**	**1.86E-07**	**1.17E-07**
SD005	2.67	0.000399	-15703.85	2.51E-02	8.97E-24
SD01	5.33	0.000292	-15103.53	5.13E-05	1.41E-19
SD04	20.5	0.000569	-14416.83	7.85E-04	4.65E-14

Figure Legends

Figure 1. Estimates of historical effective population size (N_e) obtained from linkage disequilibrium between SNPs (software GONE, panel A), or from the site frequency spectrum of variants (software Stairway Plot2, panel B). For this latter, the thick lines are median values and the thin dotted lines are the 95% confidence limits, with purple lines denoting the results using the silent sites and red lines those using the synonymous sites. The vertical blue dotted line indicates the time when the populations was captured and maintained in the laboratory since then. The horizontal green dotted line indicates the total number of individuals maintained in the laboratory population.

Figure 2. Relationship between the mean nucleotide diversity (π) and the mean recombination rate (c) in centimorgans (cM) per megabase (Mb) for 100-kb genomic windows considering the four autosomal chromosome arms, for simulation that assume an ancestral effective population size of $N_e = 10^4$. The curve shown in each graph represents the rational function fitted to the data (except for the REC model for which this function cannot be fitted and a polynomial curve is presented instead). (A) Empirical data. (B-I) Simulation results without (panels B-E) or with (panels F-I) overdominant mutations. ADD, REC: all mutations are assumed to be additive or fully recessive, respectively. NEU: only neutral mutations are assumed. M1S: mutations assuming the parameters shown in Table 1. SD005-SD08: mutations assuming the same parameters as for model M1S, and also including overdominant mutations at a rate (U_o): 0.5×10^{-7} (SD005), 1×10^{-7} (SD01), 2×10^{-7} (SD02), 4×10^{-7} (SD04), 6×10^{-7} (SD06), 8×10^{-7} (SD08). Simulation data is based on the average of 10 replicates.

Figure 3. Rational function fitted to the mean values of nucleotide diversity (π) with respect to the mean recombination rate (c) in centimorgans (cM) per megabase (Mb) for 100-kb genomic windows considering the four autosomal chromosome arms, for simulation that assume an ancestral effective population size of $N_e = 10^4$. (A) Empirical (EMP) data and models excluding overdominant mutations, as shown in Table 1. (B) Empirical (EMP) data, model M1S excluding overdominant mutations, and models assuming the same

parameters as for model M1S, and also including overdominant mutations at a rate (U_o): 0.5 × 10^{-7} (SD005), 4 × 10^{-7} (SD04), 8 × 10^{-7} (SD08).

Figure 4. Relationship between the mean nucleotide diversity (π) and the mean recombination rate (c) in centimorgans (cM) per megabase (Mb) for 100-kb genomic windows considering the four autosomal chromosome arms, for simulation which assume an ancestral effective population size of $N_e = 10^5$. The curve shown in each graph represents the rational function fitted to the data. (A) Empirical data. (B) Simulation results for model M1S without overdominant mutations. (C-D) Models assuming the same parameters as for model M1S, and also including overdominant mutations at a rate (U_o): 0.05 × 10^{-7} (SD005) and 0.1 × 10^{-7} (SD01). Simulation data is based on the average of three replicates.

Figure 5. Average nucleotide diversity (π; panel A) and linkage disequilibrium between consecutive loci (r^2; panel B) for a range of simulated overdominant mutation rates, ranging from $U_o = 0.5$ to 8 × $10^{-7,}$, with the x-axis indicating the mean number of overdominant segregating mutations (n_o) for each overdominance mutation rate. Results refer to simulations that assume an ancestral effective population size of $N_e = 10^4$. The values of π refer to 100-kb genomic windows with average recombination rate $c < 0.25$ cM/Mb. Dots indicate the mean π or r^2 based on the ten simulated replicates, and bars the 95% confidence intervals. The green dots refer to the empirical data with confidence limits obtained by bootstrapping, the blue dots correspond to the simulation results assuming the mutation model M1S without overdominance, which parameters are shown in Table 1. The red dots refer to the models assuming the same parameters as for model M1S, but also including overdominant mutations at a rate (U_o) ranging from 0.5 × 10^{-7} to 8 × 10^{-7}.

Figure 6. Mean number (n) and average frequency (q) of neutral (subscript *neu*), partially recessive deleterious (*del*), additive slightly deleterious (*sdel*), lethal (*let*), adaptive (*adap*) and overdominant (o) mutations. Results refer to simulations that assume an ancestral effective population size of $N_e = 10^4$. The blue dots correspond to the simulation results assuming the mutation model M1S without overdominance, which parameters are shown in Table 1. The red dots refer to the models assuming the same parameters as for model M1S, but also including overdominant mutations at a rate (U_o) ranging from 0.5 × 10^{-7} to 8 × 10^{-}

^{7}, with the x-axis indicating the mean number of overdominant segregating mutations (n_o) for each overdominance mutation rate. Results are based on 10 simulation replicates and bars indicate 95% confidence intervals.

Figure 7. Changes of inbreeding load (B, panel A), additive variance (V_A, panel B) and dominance variance (V_D, panel C) for models assuming the same parameters as for model M1S (parameter in Table 1), but also including overdominant mutations occurring at different rate U_o, leading to different numbers of segregating overdominant mutations (n_o). Results refer to simulations that assume an ancestral effective population size of $N_e = 10^4$. Red dots give the overall values contributed for all kind of loci, with the x-axis indicating the mean number of overdominant segregating mutations (n_o) for each overdominance mutation rate. Blue dots and lines indicate the contribution from segregating non-overdominant loci. Results are based on 10 simulation replicates.

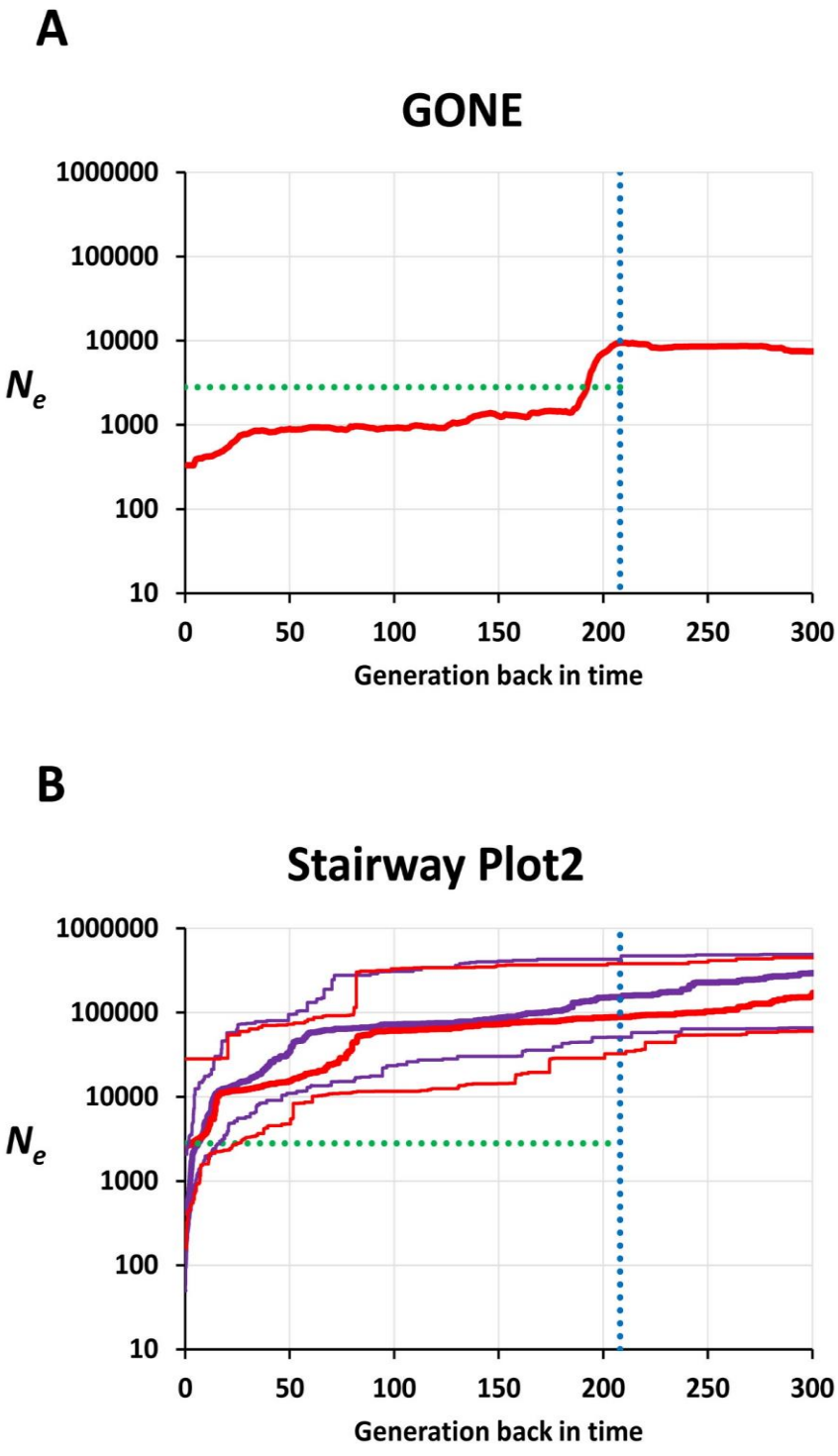

Figure 1
161x247 mm (x DPI)

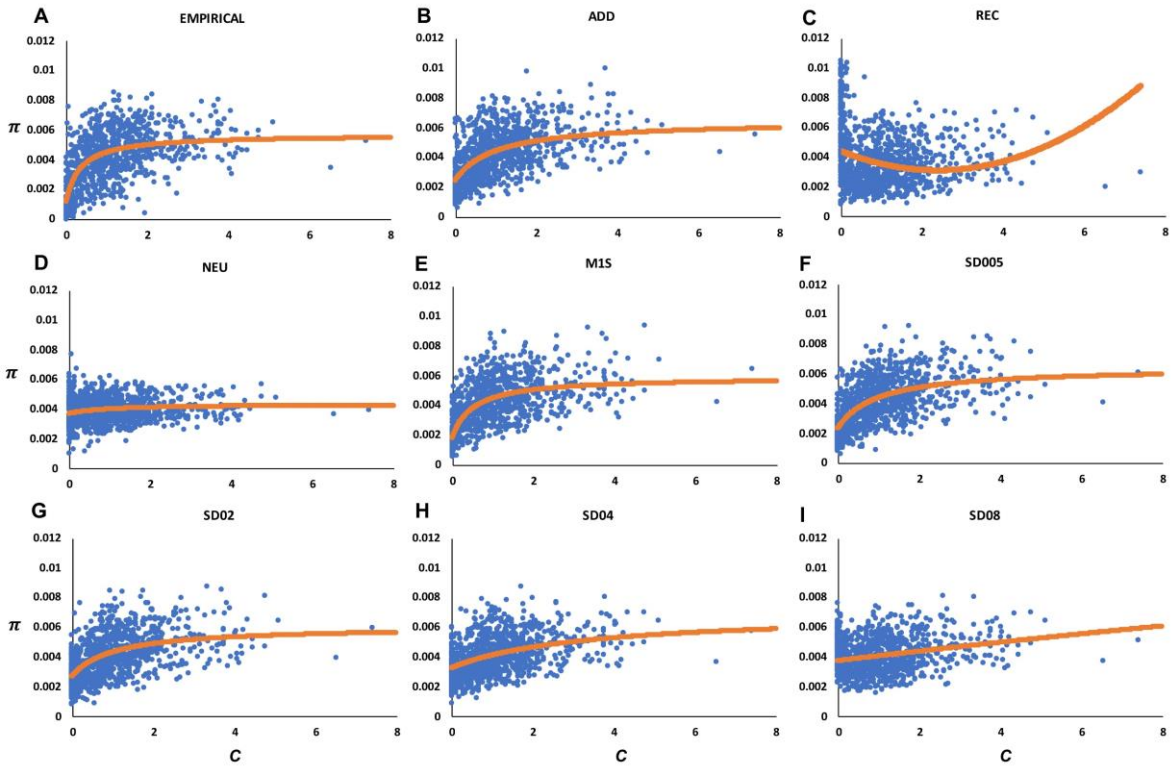

Figure 2
403x266 mm (x DPI)

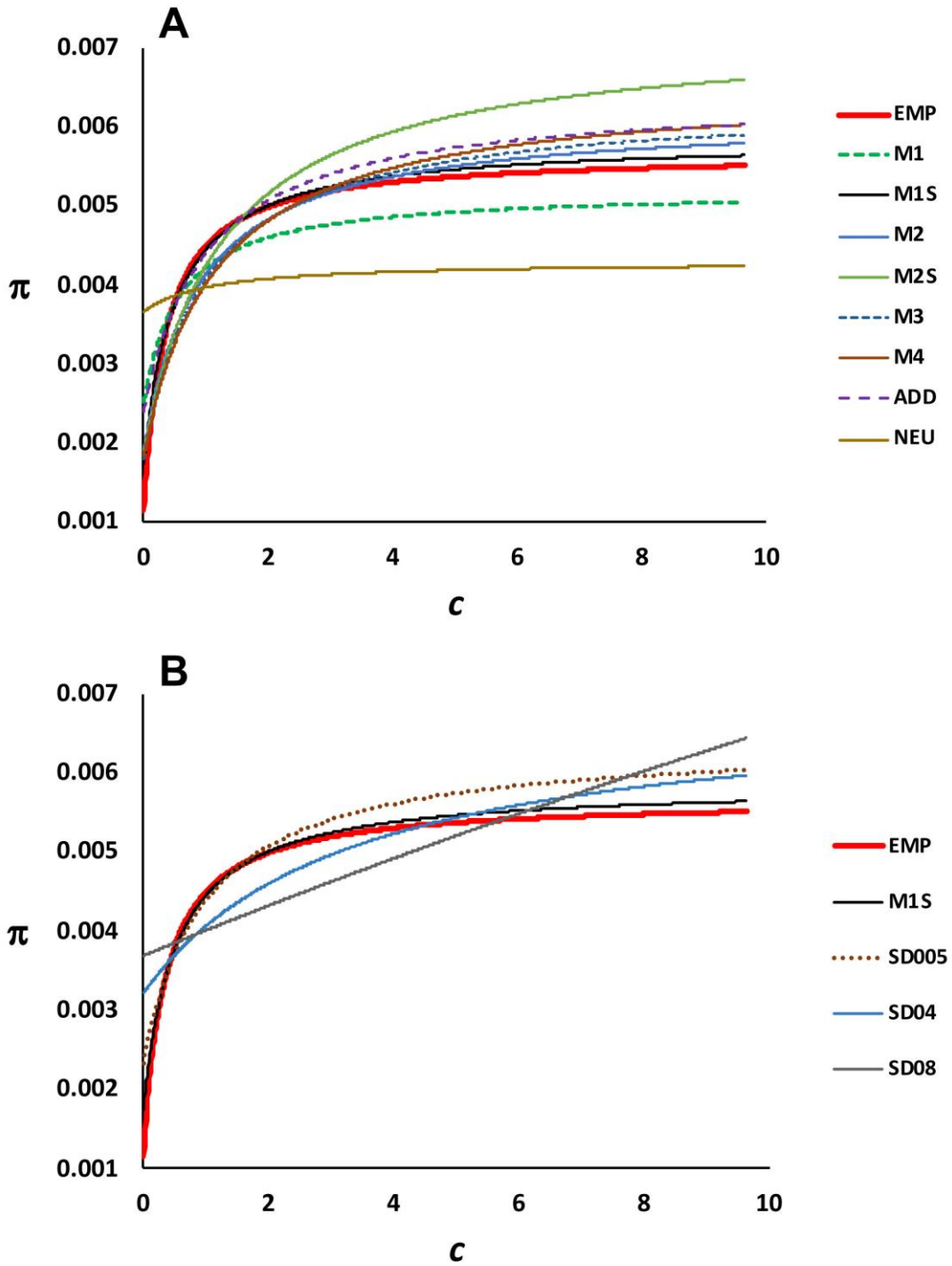

Figure 3
193x239 mm (x DPI)

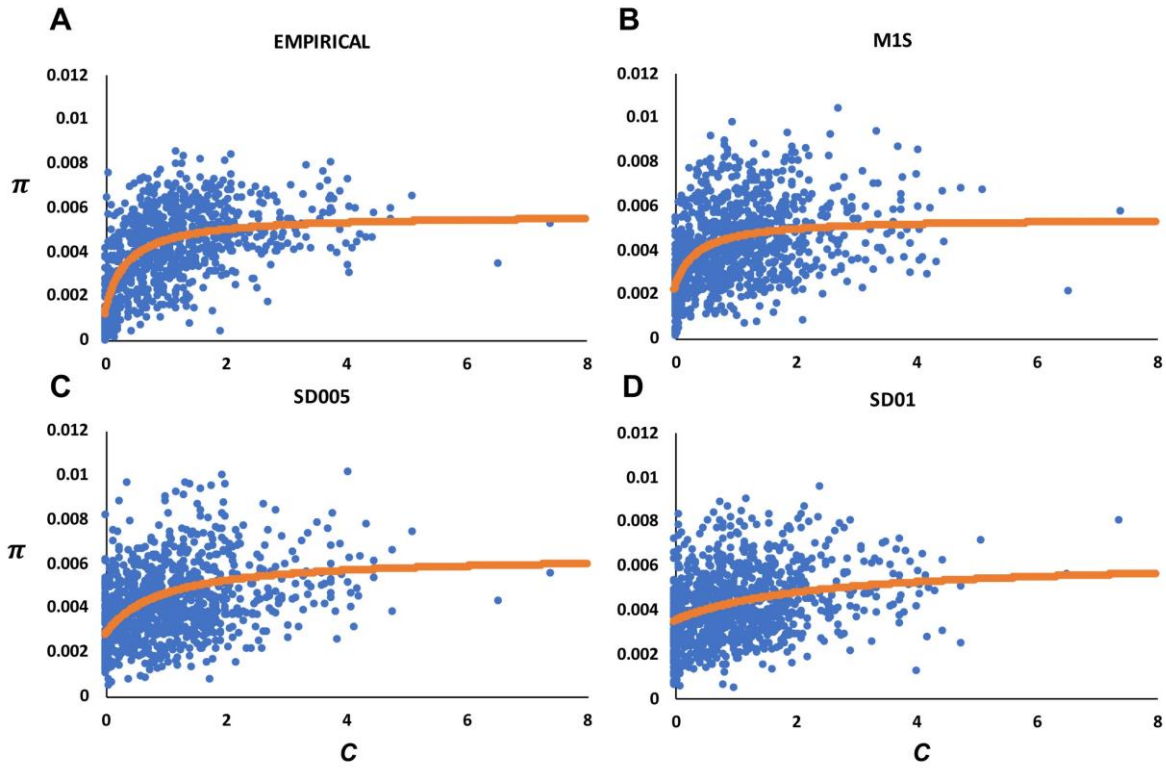

Figure 4
271x182 mm (x DPI)

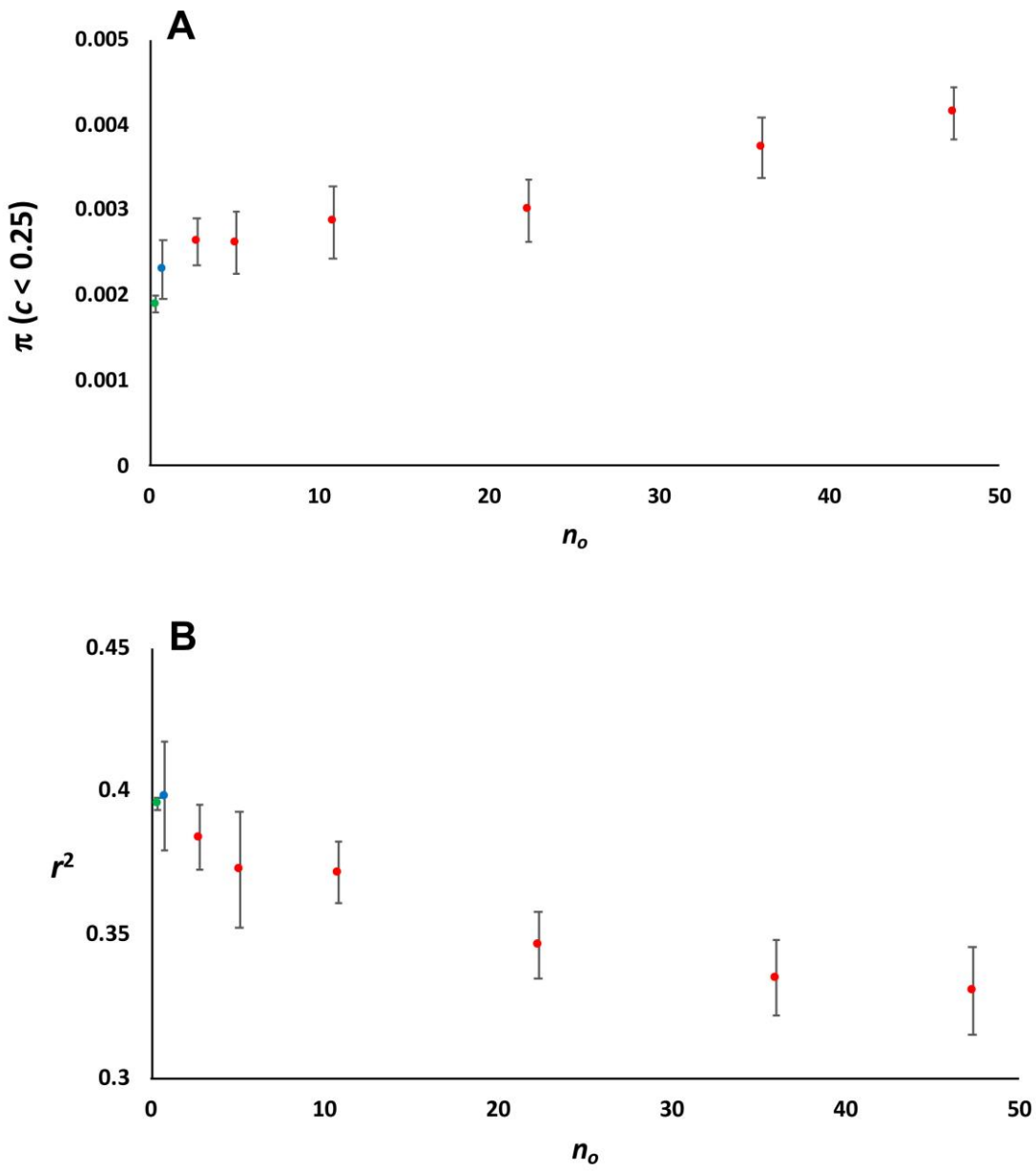

Figure 5
220x232 mm (x DPI)

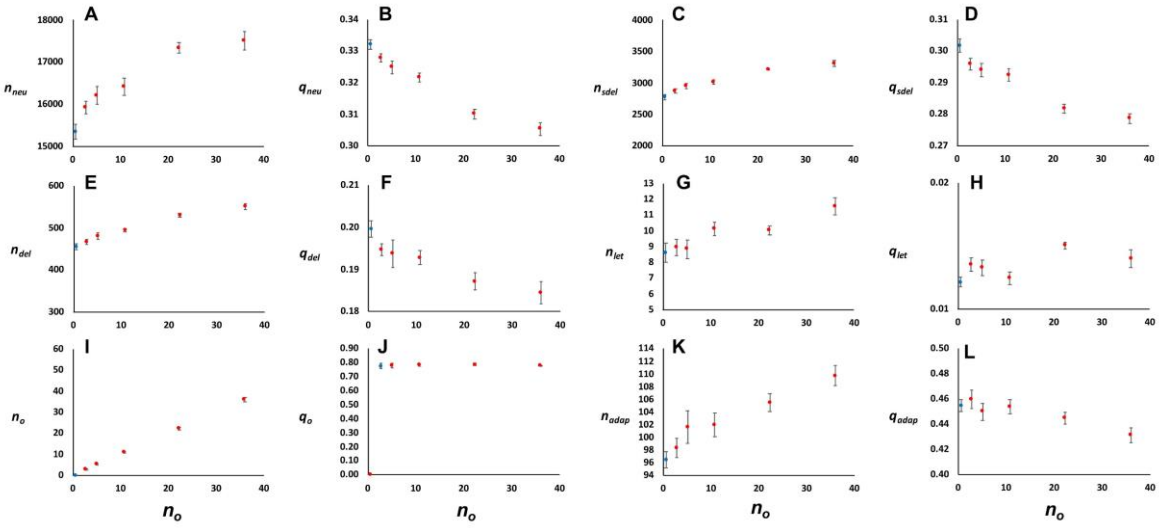

Figure 6
477x217 mm (x DPI)

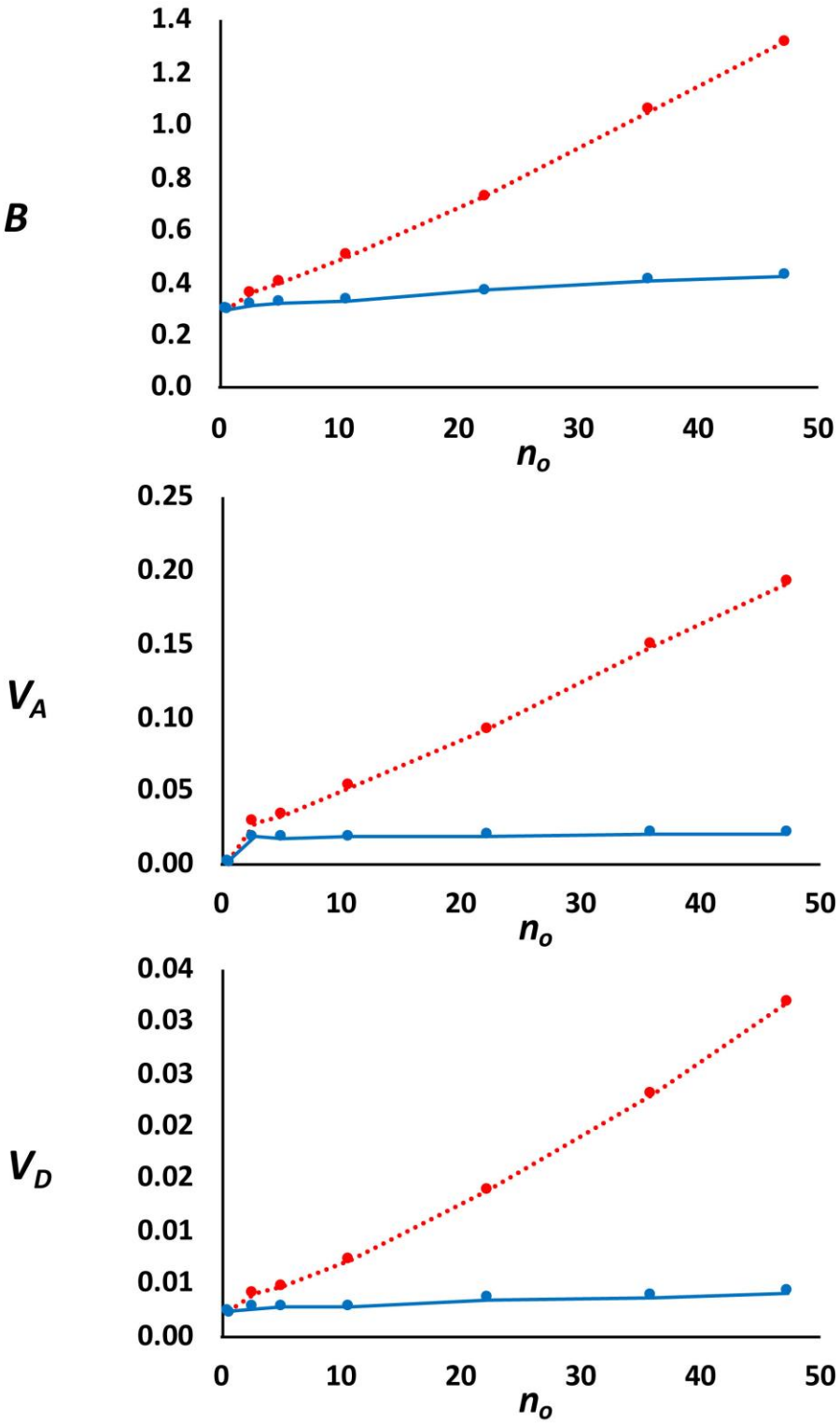

Figure 7
162x250 mm (x DPI)